# Surface and thin film structural determinations from combined Photoelectron Diffraction and Grazing Incidence X-ray Diffraction experiments

Alberto Morgante
Laboratorio TASC-INFM Trieste
e
Dipartimento di Fisica Università di Trieste

Surface and thin films crystallography.

Experimental techniques:
Low Energy Electron Diffraction (LEED)
High Energy Electron Diffraction (RHEED)
He Atom Scattering (HAS)
PhotoElectron Diffraction (PED)
Grazing Incidence X-ray Diffraction (GIXD)

Surface sensitivity: short mean free path (LEED, PED, HAS) or grazing incidence (RHEED e GIXD).

LEED:
cheap experimental apparatus but dynamical calculations

GIXD: Kinematic scattering calculations $\Rightarrow$ large structural parameter space
**but** synchrotron radiation, high experimental apparatus complexity.

For thin films: GIXD variable penetration depth study of buried interfaces.

# In plane X- Ray Diffraction measurements

In plane measurements: grazing incidence, grazing emission.

In plane structural parameters determination.

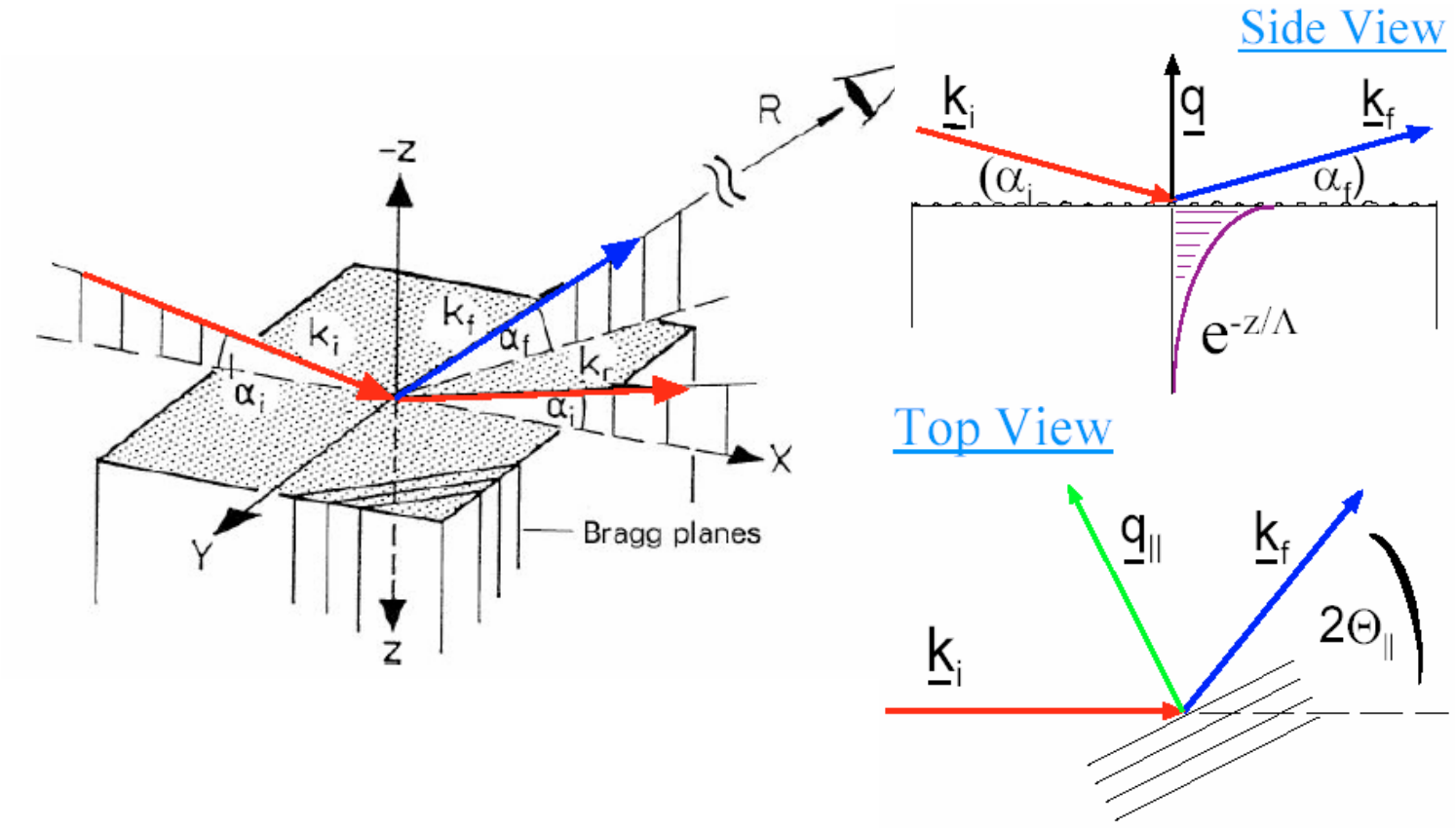

Rod scan: Grazing incidence
Constant Q transfer
variable exit angle $Q_z$ variation
Out of plane structural determination

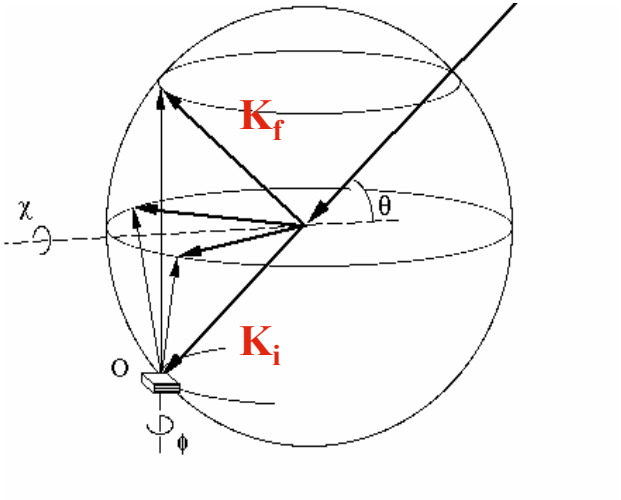


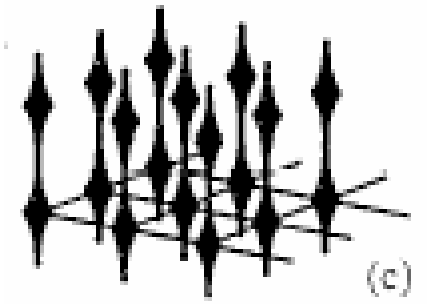

# ALOISA beamline

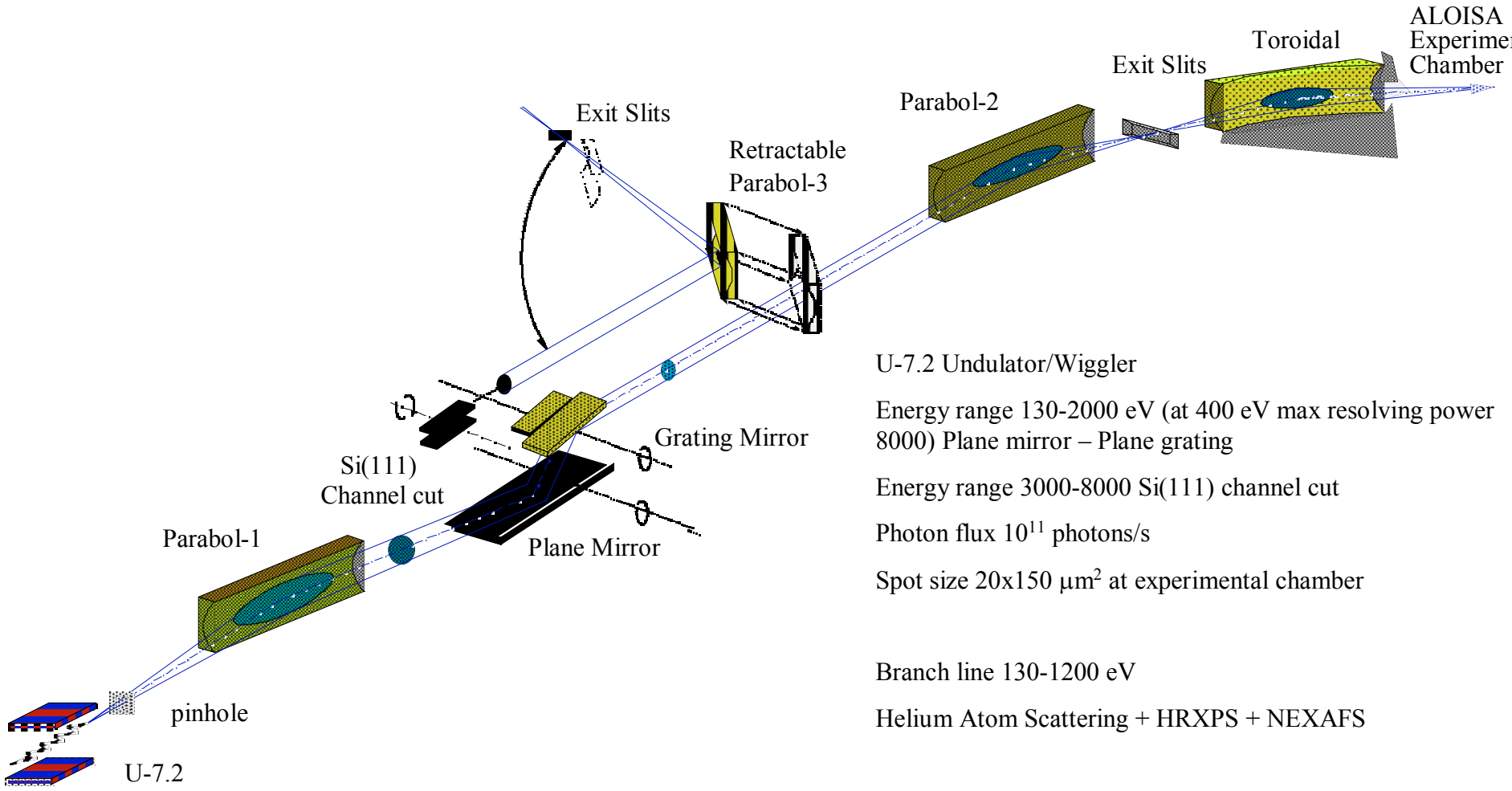


U-7.2 Undulator/Wiggler

Energy range 130-2000 eV (at 400 eV max resolving power 8000) Plane mirror – Plane grating

Energy range 3000-8000 Si(111) channel cut

Photon flux $10^{11}$ photons/s

Spot size 20x150 $\mu m^2$ at experimental chamber

Branch line 130-1200 eV

Helium Atom Scattering + HRXPS + NEXAFS

# Experimental apparatus

ALOISA

**High Resolution Photoemission Spectroscopy**
**X-Ray Photoelectron Diffraction**
**Grazing Incidence X-Ray Diffraction**
**X-Ray Reflectivity**
**Absorption Spectroscopy**

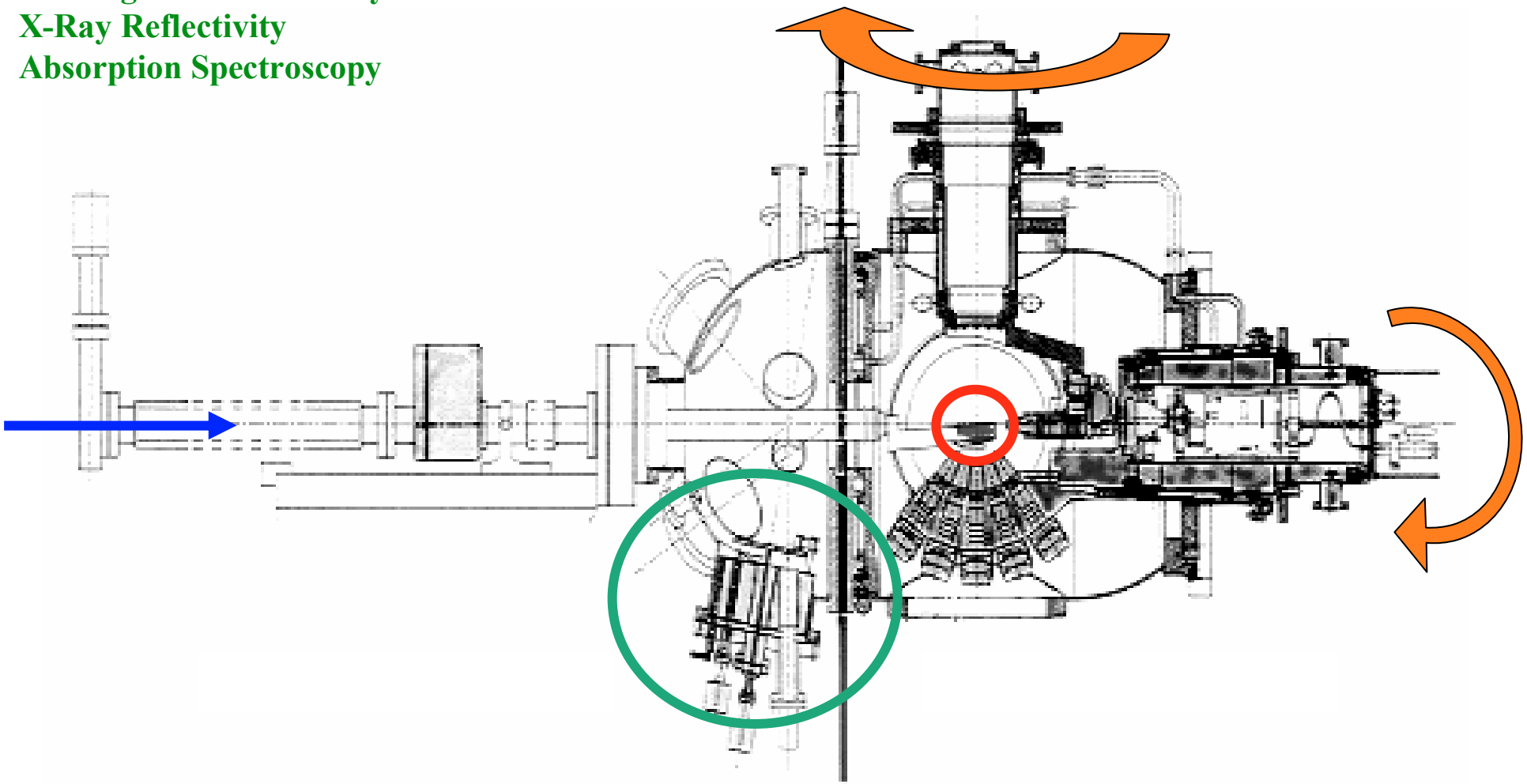

Preparation chamber

Experimental chamber

Fe magnetic properties depend on its lattice cell

Fe FM: bcc, a = 2.87 Å

Au: fcc, a = 4.08 Å
Ag, fcc, a = 4.07 Å
half diagonal = 2.88 Å

Fe superFM: fcc, a = 3.65 Å

$Cu_3Au$: fcc, a = 3.75 Å

Fe AF: fcc, a = 3.59 Å

Cu: fcc, a = 3.61 Å
Ni, fcc, a = 3.52 Å

Suitable choice of the substrate allows to grow thin Fe films with different structures

# Fe/Cu(100)

**Structure:** 1-4 ML pseudomorphic FM fcc, Fe on hollow
4-10 MLtopmost bilayer FM fcc; inner layers
AF fcc
> 10 ML FM bcc (110), Fe on bridge

**Morphology:** 1-10 MLlayer-by-layer growth
> 10 MLVolmer-Weber growth

**Magnetism:** < 2 MLno magnetic signal
2-10 ML⊥ magnetization
> 10 ML// magnetization

10 ML → Martensitic fcc to bcc transition
→ Spin Re-Orientation transition

# $Fe/Cu_3Au(100)$

**Wuttig** (LEED I-V, MOKE)

Prep. 2 ML pre-deposited at LT

Structure:

> 3.5 MLbct

> 5-6 MLbcc

Morphology: - - -

Magnetism:

1.1 ML ⊥ magnetiz. onset

2.3 ML⊥ to // SRO transition

> 6 MLeasy axis <110>

**Kirschner** (STM, MOKE)

Structure:

<3.5 MLpseudomorphic fct

3.5-6 MLfct + bct

> 10-12 MLbcc

Morphology:

1.1 ML (three levels populated)

> 2.5 ML islands elongated along <110>

Magnetism:

2.1 ML⊥ magnetiz. onset

3.3 ML⊥ to // SRO transition

No correlation between SRO and structural modifications

SRO transition ⇔ bct phase

**Low Temperature Growth**

**Wuttig Kirschner**

anticipated ⊥ onset 0.9 ML anticipated ⊥ onset: 1.1 ML

delayed SRO: 3.3 ML delayed SRO: 5.5 ML

anticipated bcc delayed bct: 5.5 ML

(films annealed after dep.)

# $Fe/Cu_3Au(100)$ GROWTH

## X-ray reflectivity during deposition

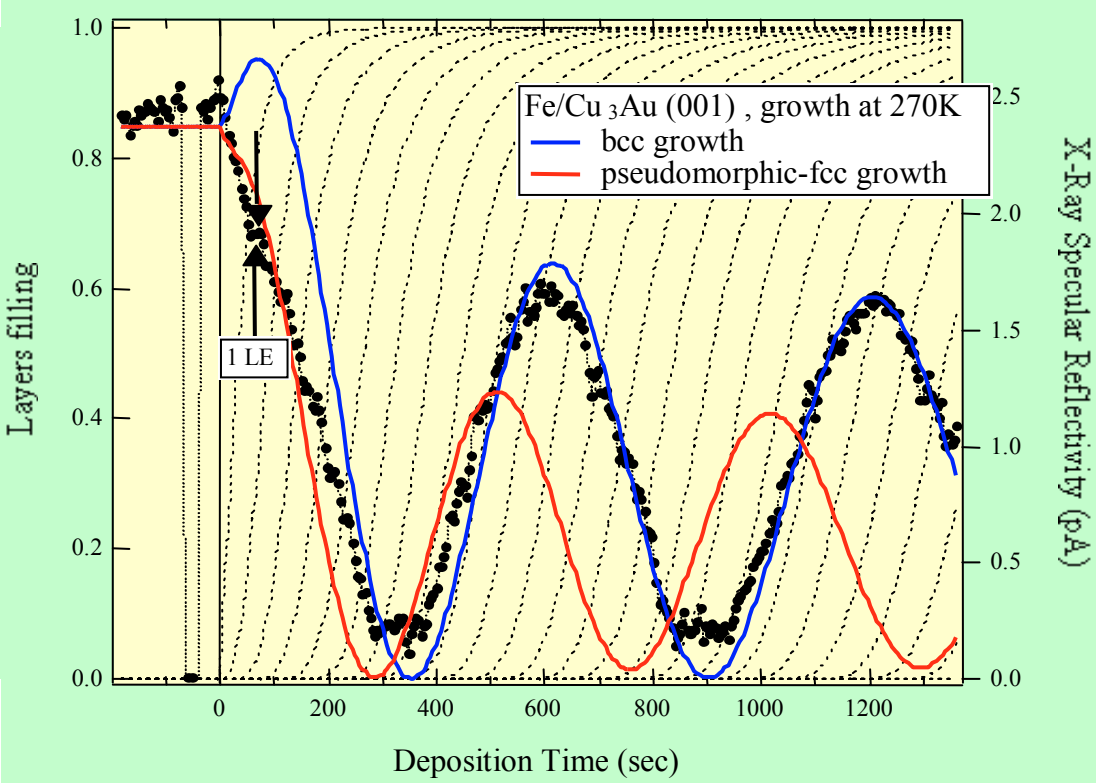


X-ray reflectivity during Fe deposition
X-ray specular intensity at fixed energy and angle
Accurate thickness determination
Interfaces roughness determination
Morphology
Fit to a bcc model deposition only works beyond 10 ML

# In plane Surface X-ray Diffraction

Radial scan across the substrate (2,0,0) peak; energy scans

γ phase appears at 10 Å and disappears at 20-25 Å

α phase appears at 15 Å and evolves towards the bcc lattice parameter beyond 20 Å

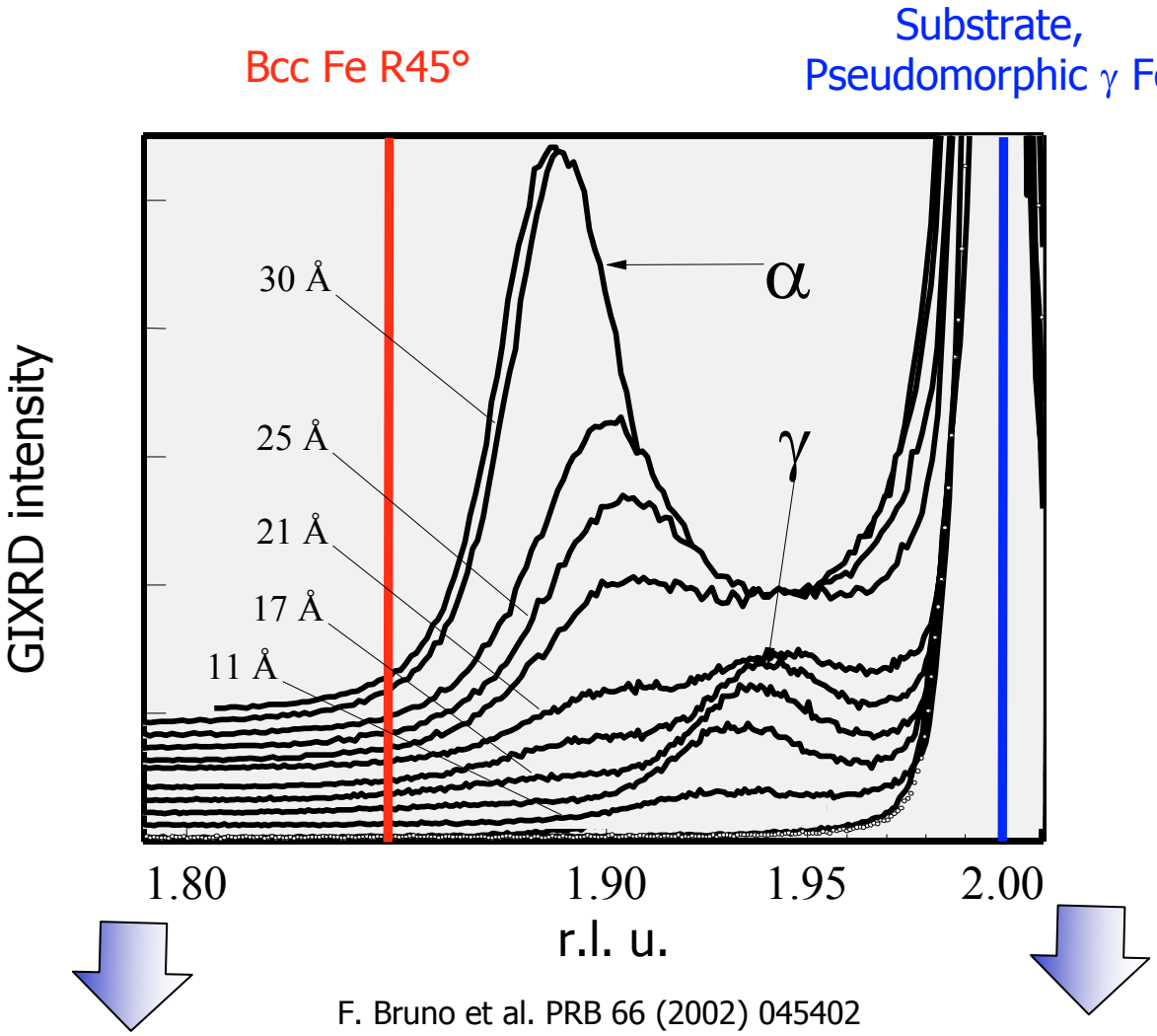


F. Bruno et al. PRB 66 (2002) 045402

Strain is gradually released with increasing film thickness

# Electron Diffraction from Fe LMM Auger (698 eV)

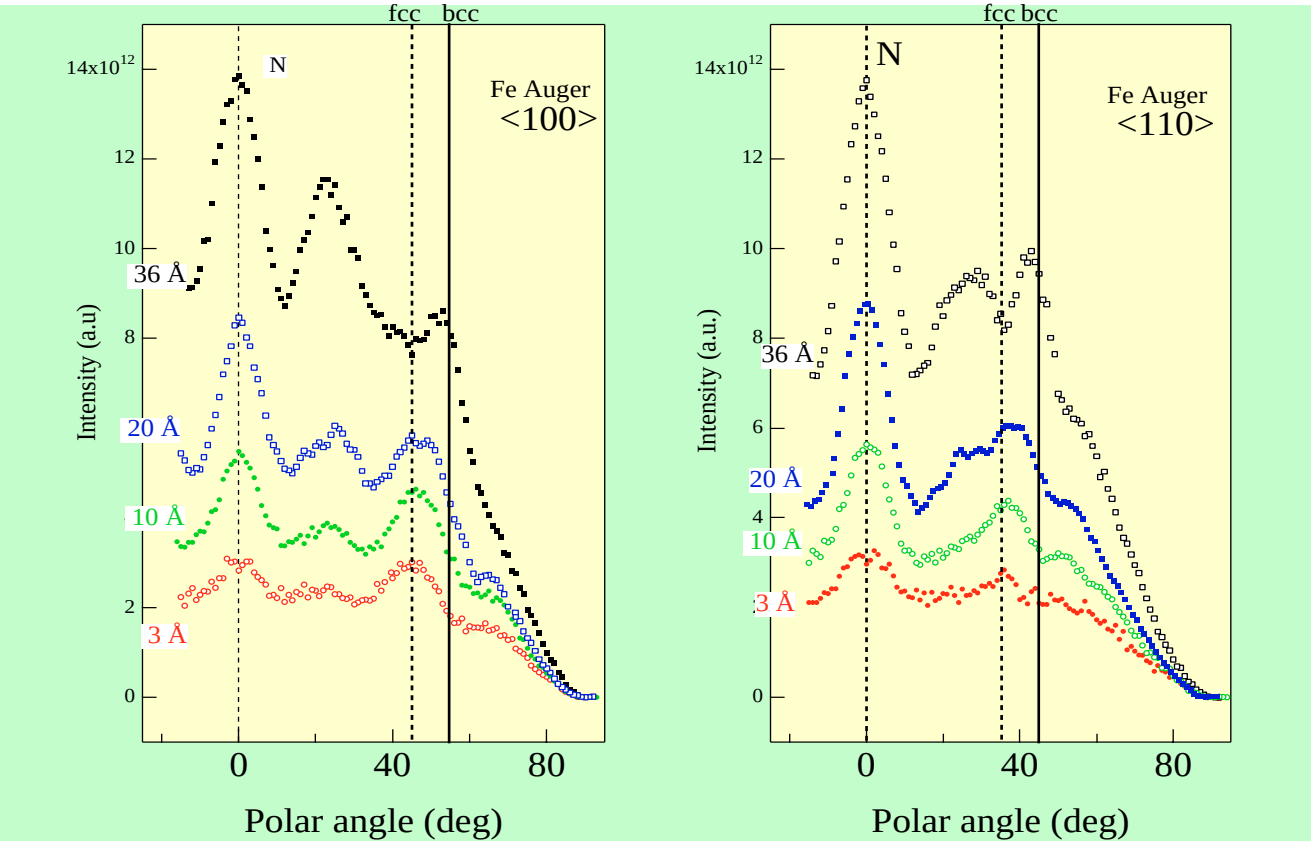


Out of plane structural determination

Polar scans taken at fixed incidence angle by rotating the analyzer in the scattering plane (TM polarization)

Gradual shift of the forward focussing peak from fcc to bcc

Data comparison to multiple scattering calculations

Isotropic background calculated for given instrumental conditions (sample illumination, escape depth, emission matrix element)

Input value for lateral lattice spacing taken from XRD data

# Linear combination of three phases: pseudomorphic fcc, fct, bct

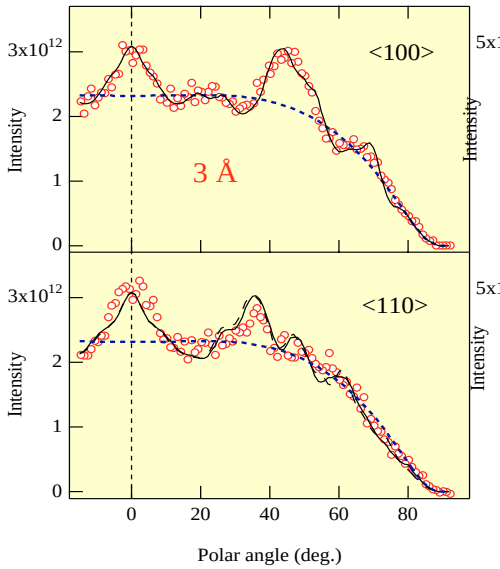


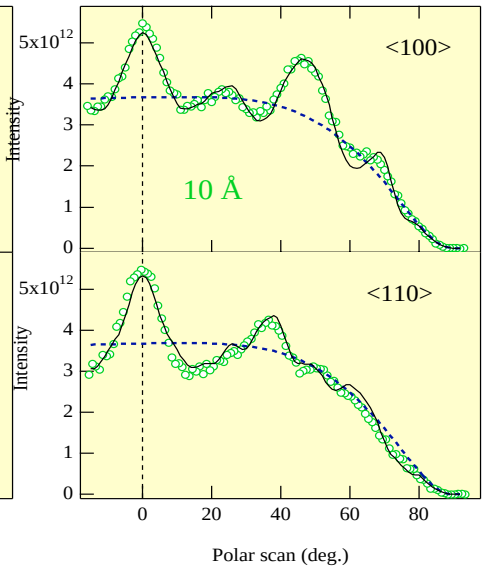


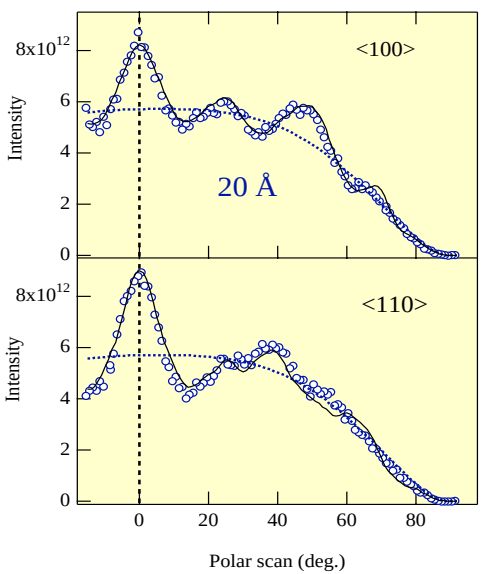


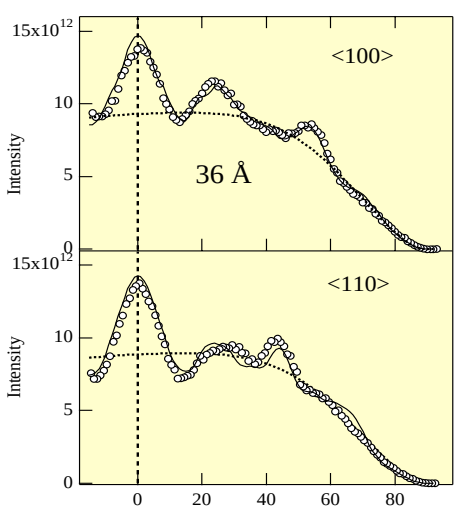


3 Å ⇒ fcc pseudo-morphic structure; slight vertical compression c=1.38

10 Å⇒ phase co-existence: fcc (60 %) + fct (40 %)

20 Å⇒ phase co-existence: fcc (40 %)+ fct (40 %) + bct (20 %)

> 30 Å ⇒ bct structure; evolution towards bcc phase

# Fcc structures are obtained by straining the bcc structure

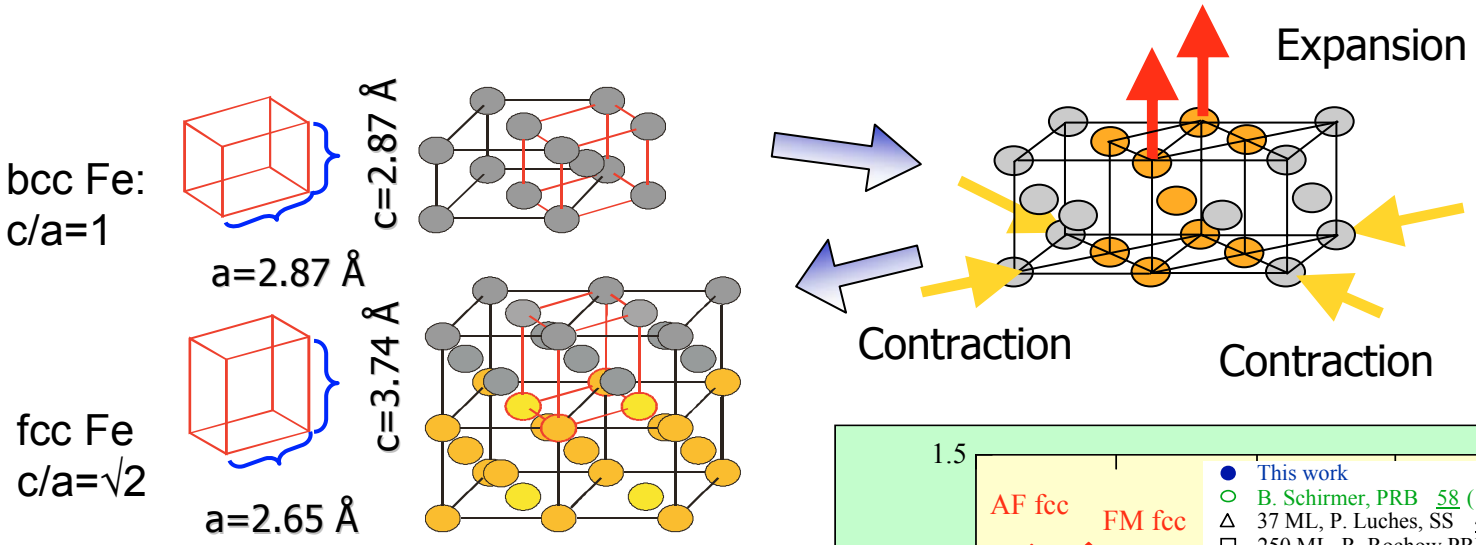


## Epitaxial plane

- Three Fe phases are seen to coexist between 10 and 20 Å
- a=2.74 Å is the maximum strain of the γ–fct phase
- At 25 Å, the α phase becomes the dominant one and it evolves towards the Fe bcc value.

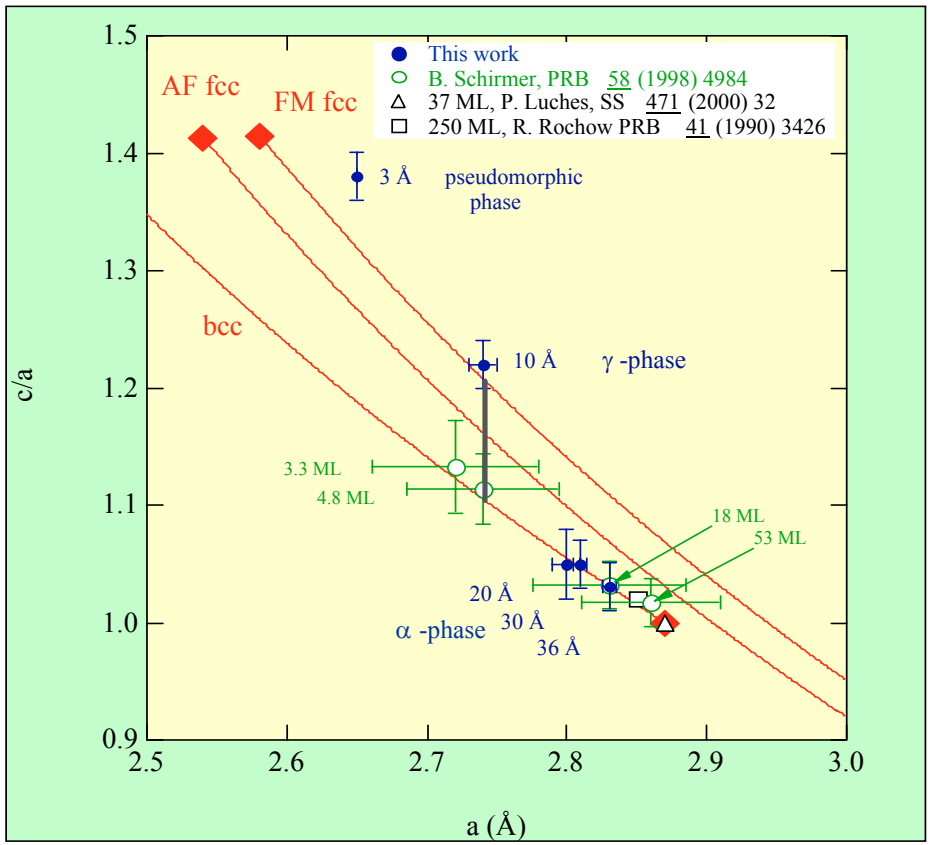

Fe films 6÷13 Å thick deposited at 150 K or 300 K, annealed at 400 K for T~10 min and cooled to room temperature (RT);

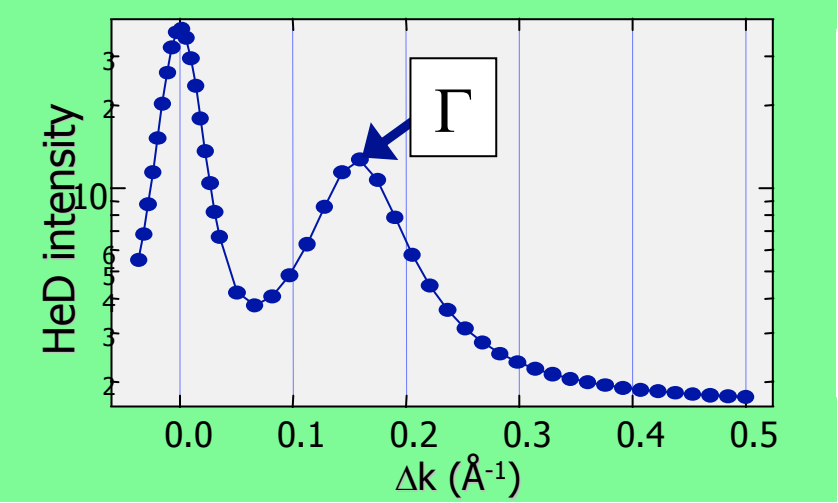


HeD pattern along [110] direction near specular region

Γ peak appears

HeD [110]

- π pseudomorphic to the substrate (a=2.65 Å);
- γ Expanded phase (a=2.78 Å);
- Δk (π- γ)=k(Γ);

LEED [110]

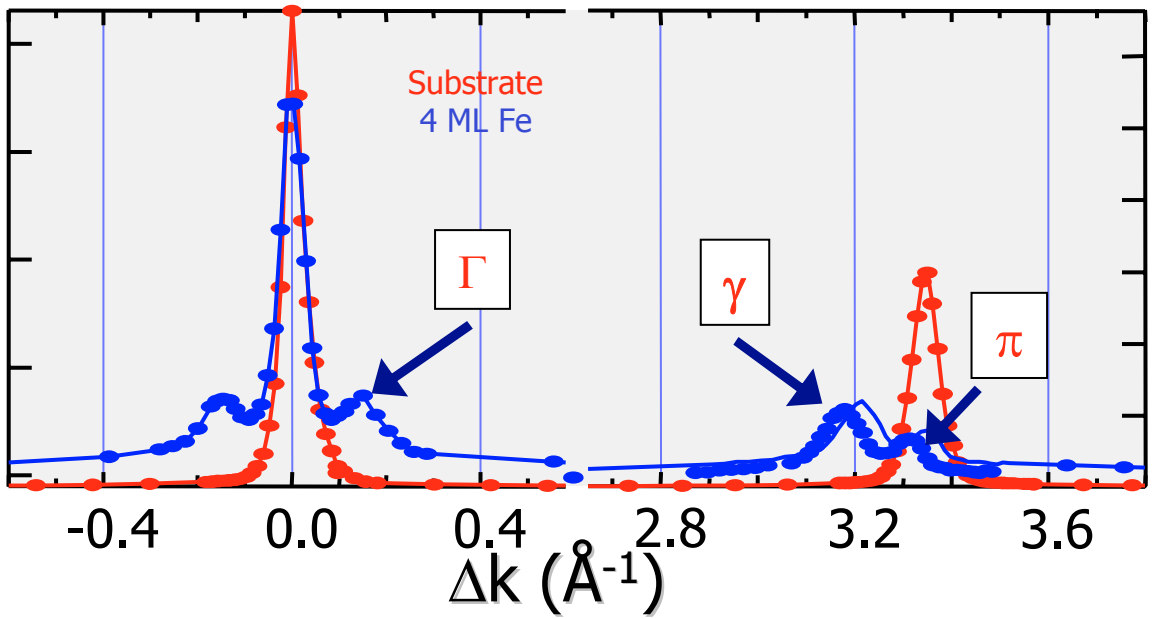

# TEMPERATURE DRIVEN REVERSIBLE BREAKDOWN OF PSEUDOMORPHISM

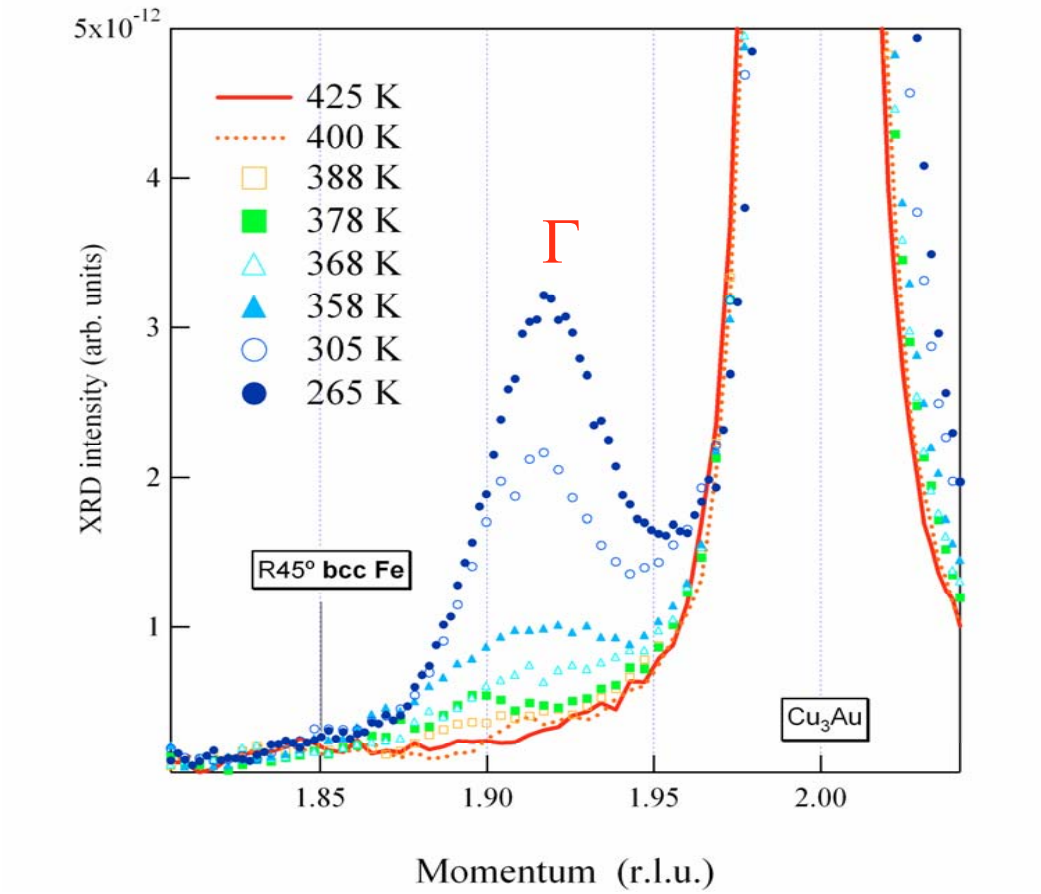


## In plane XRD

Fe film of 7.5 Å deposited at 150 K and annealed at 425 K

Radial scan along [100]

Pseudomorphic Fe contributes to $Cu_3Au$ bulk peak. Rod scans clearly indicate the presence of pseudomorphic layers.

Γ peak **reversibly** disappears

## Auger Electron Diffraction

Fe Auger LMM (KE 698 eV) electron peak

High temperature phase ⇒ better defined angular structures

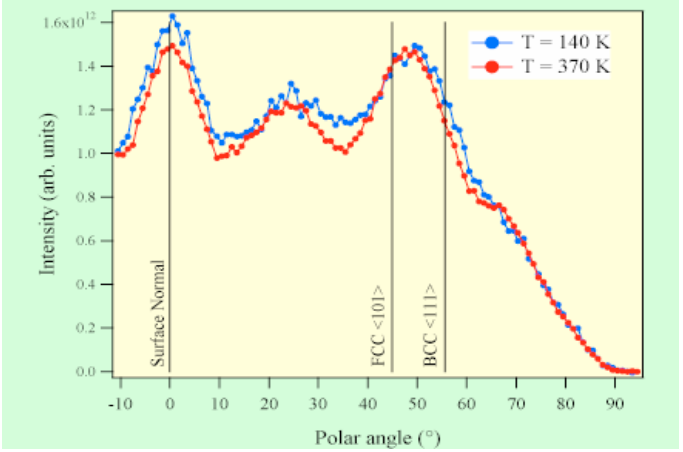

Films grown on bulk substrate adopt substrate structure and lattice constant (**PSEUDOMORPHISM**) in early stages of growth and gradually relax towards unstrained structure with increasing thickness

Elastic energy is accumulated during pseudomorphic growth

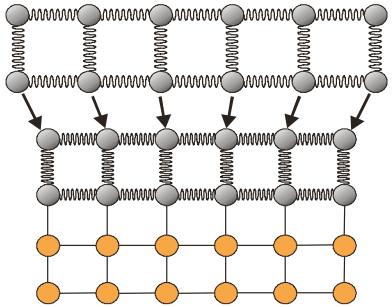

Stress is released by the formation of edge dislocations

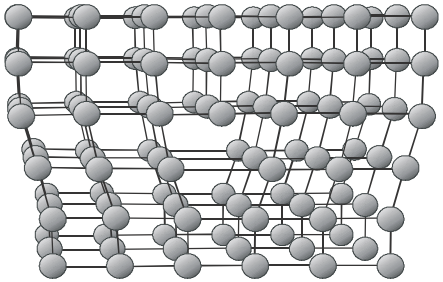

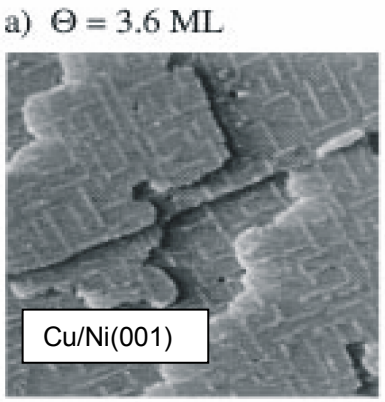


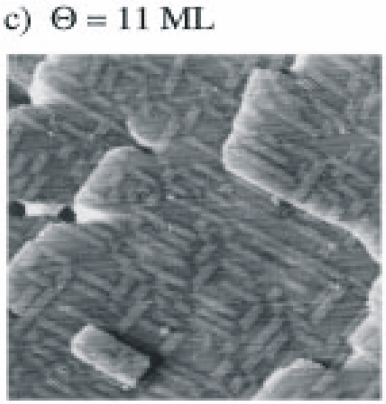


B. Müller et al. PRL 76 (1996) 2358

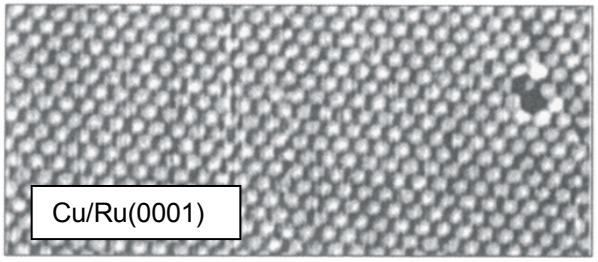


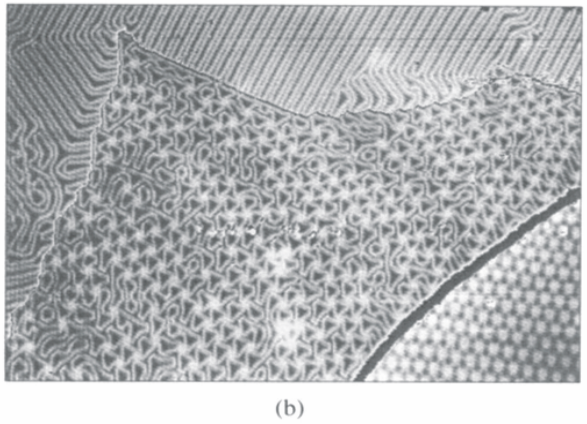


C. Gunther et al. PRL 74 (1995) 754

- The γ phase and the dislocation network disappear upon annealing at 400 K;
- Upon cooling back to RT both the γ and the dislocation network REVERSIBLY reappear → **PHASE TRANSITION**;
- The phase transition is observable within the 6÷13 Å Fe thickness range;
- The transition temperature increases from T=345 K for 6 Å Fe to T=380 K for 11 Å Fe;
- No correlation with magnetic properties of the film is observed;

# Modelling the transition and its driving force

Phase coexistence ⇒ 1st order phase transition

## Gradual enlargement of pseudomorphic patches

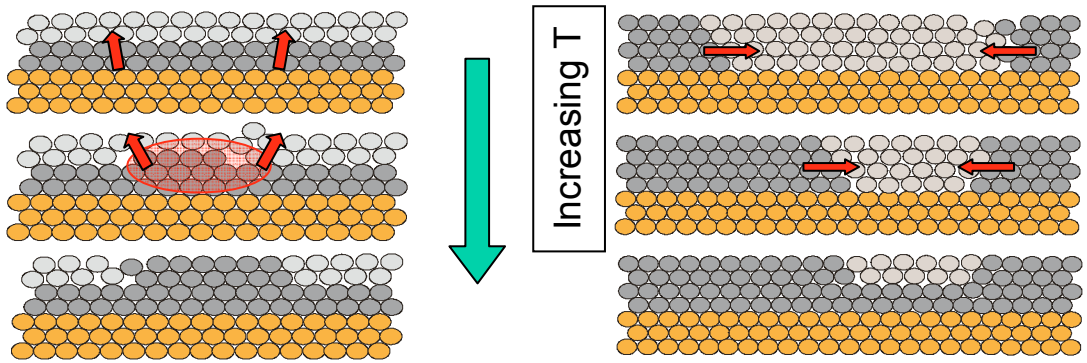


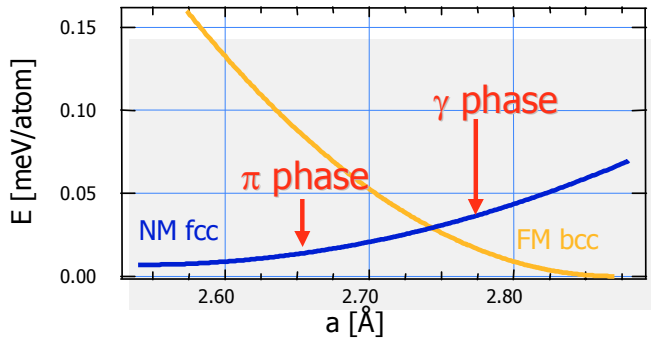


## Elastic energy must play a dominant role

Temperature dependent misfit:
- Linear thermal expansion coefficient $\alpha(Cu_3Au)=1.9\cdot10^{-6}$ $K^{-1}$
- Linear thermal expansion coefficient $\alpha(Fe)=1.1\cdot10^{-6}$ $K^{-1}$

**Misfit decreases with temperature!!**
**Critical thickness for pseudomorphism breakdown increases**

**Phase stacking or phase mixing ?**
XRD vs Tilt
In plane X-ray Diffraction

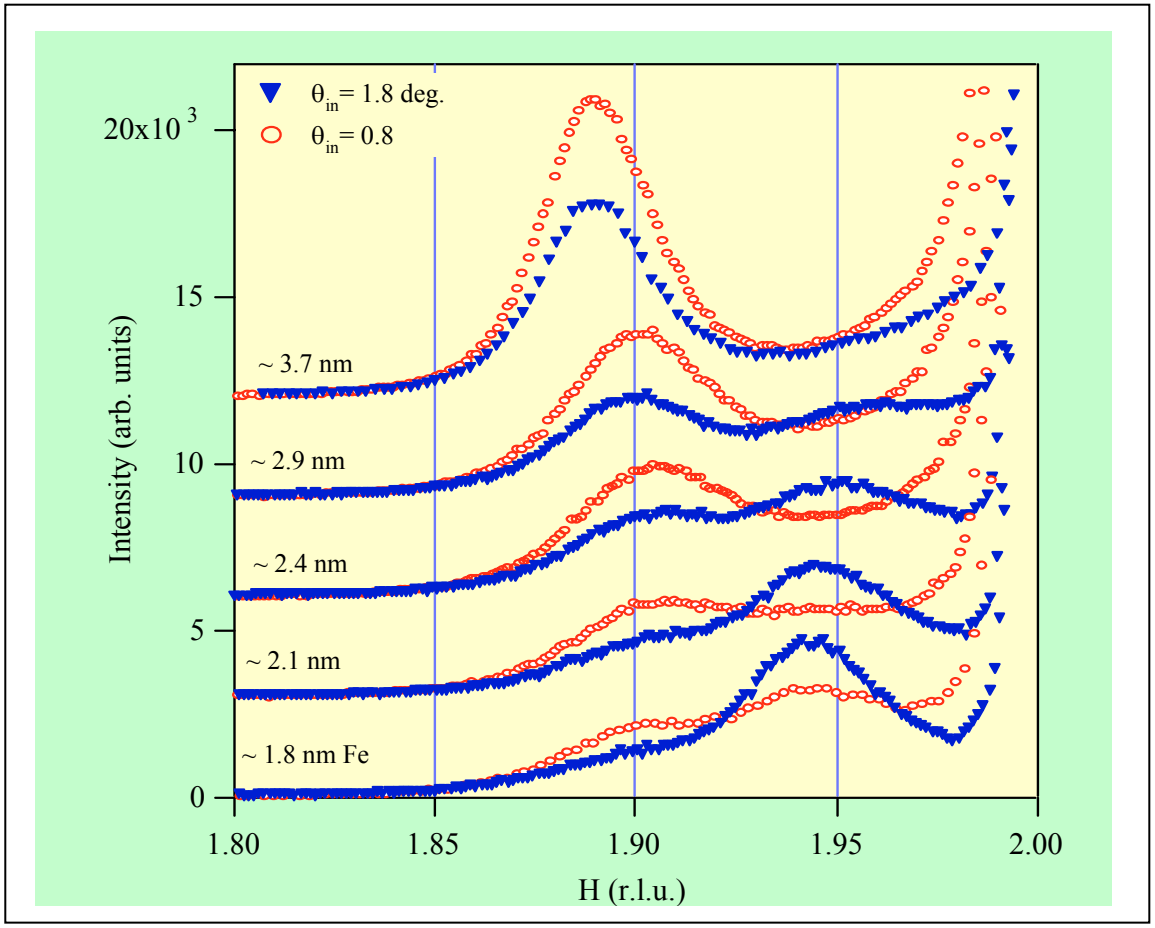


Grazing angle below the critical angle (red markers):
the α (bct) phase is enhanced
Grazing angle above the critical angle (blue markers):
the α' (fct) phase is enhanced

⇓

The bct Fe phase is formed on top the fct one
The two phases coexist in a wide thickness range

**Phase stacking or phase mixing ?**

Cu, Au electron diffraction vs direction

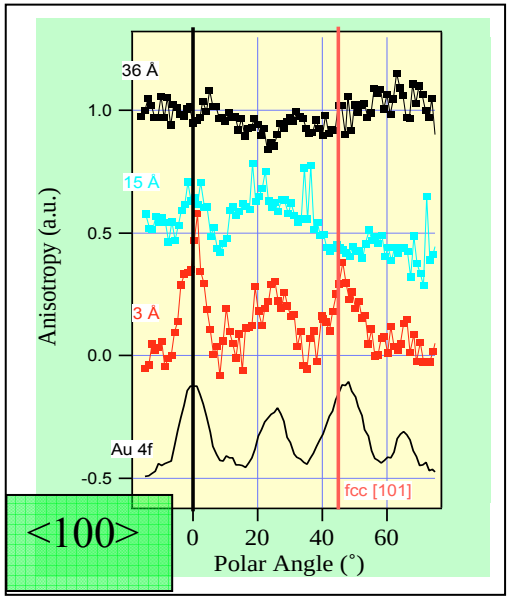


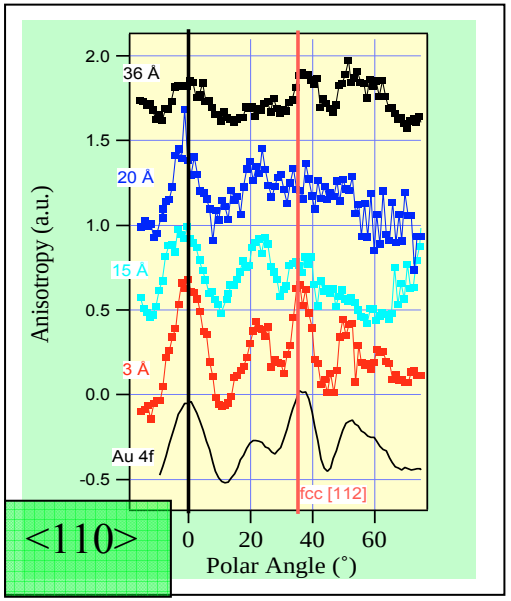


Au $4f_{7/2}$
Ek=895 eV

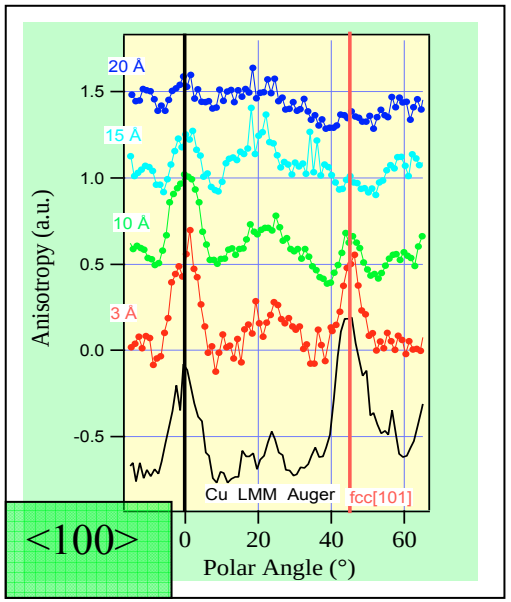


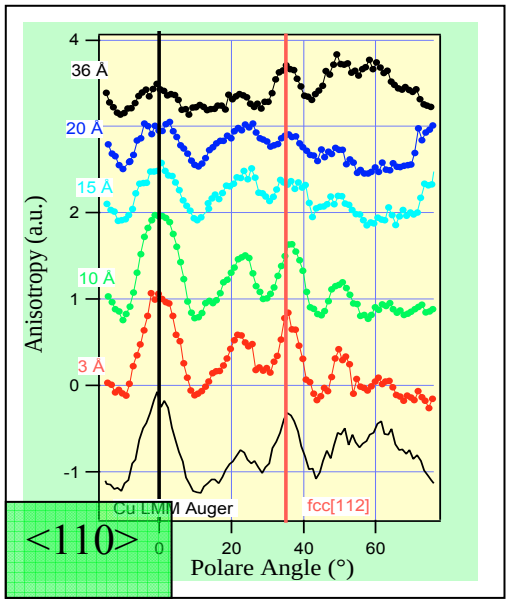


Cu LMM
Ek=914 eV

The Cu and Au anisotropy does not disappear along <110>

The Cu and Au anisotropy always corresponds to an fcc phase

⇓

The film displays a rippled morphology with troughs along <110>

# Low temperature Fe bi-layer islands

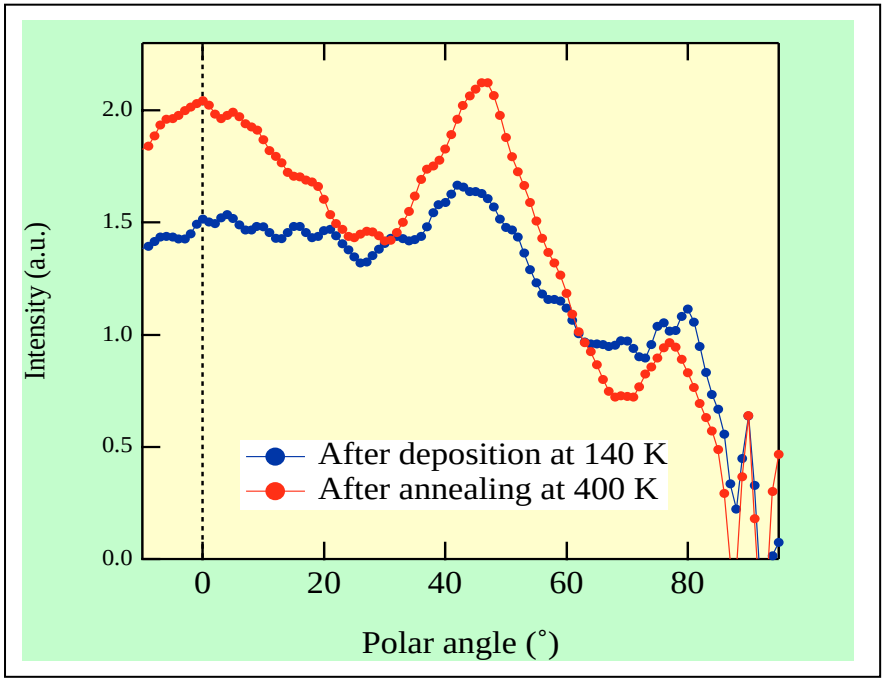


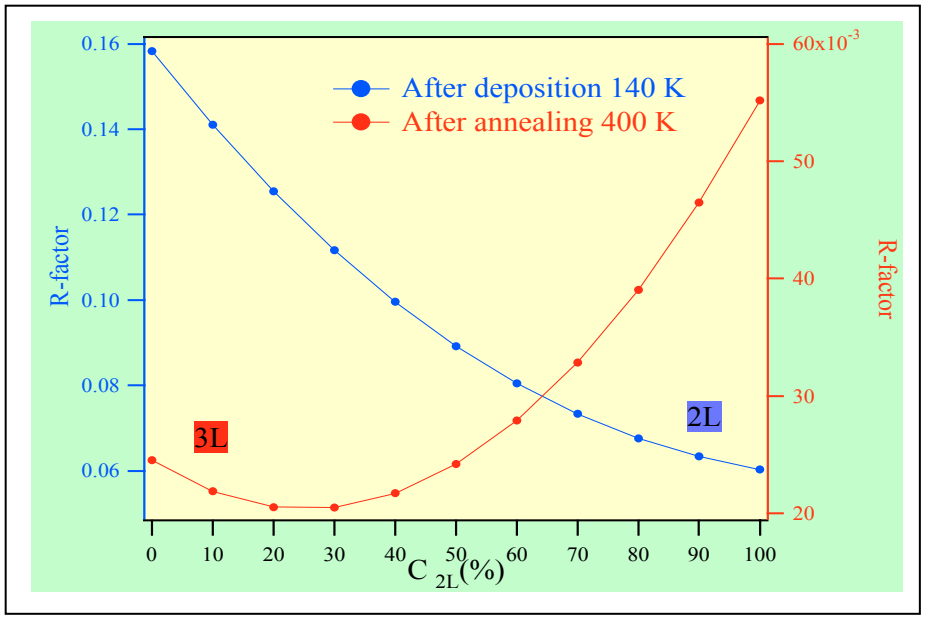


Deposition at 140 K ⇒ Flat bi-layer islands are formed
Annealing to 400 K ⇒ Third layer is formed
Fit to multiple scattering calculations, assuming the lateral lattice spacing to be equal to the substrate one

# Low temperature Fe bi-layer islands

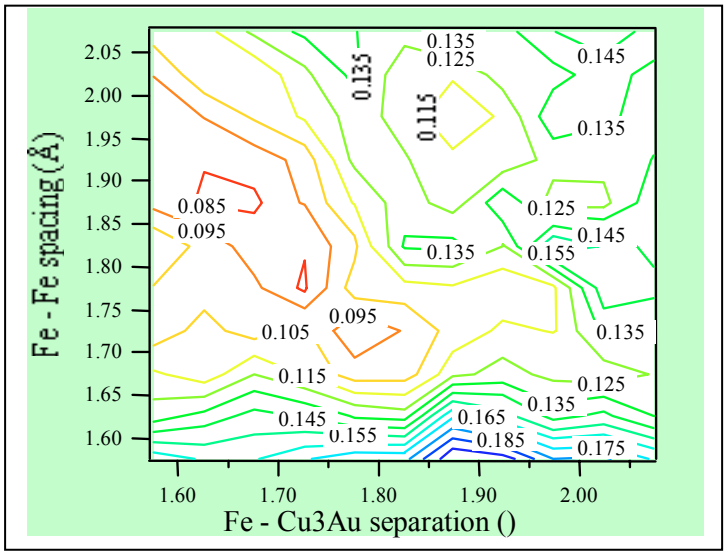


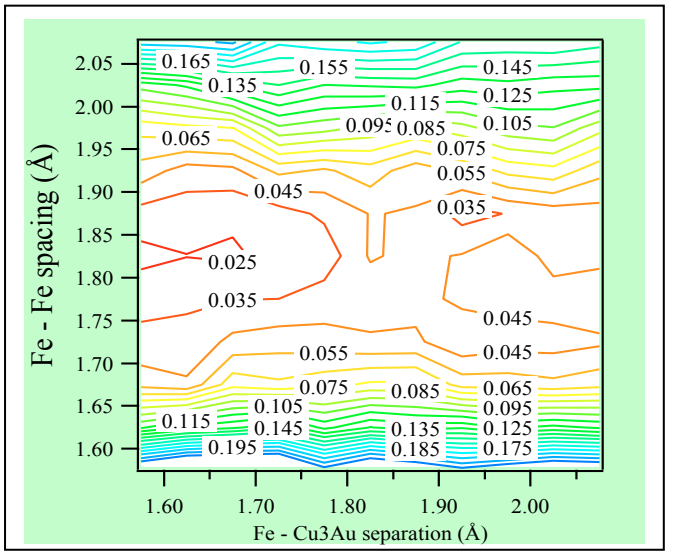


**Bilayer islands**
**Fe-Fe = 1.87 Å**
**Fe-Cu3Au = 1.68 Å**

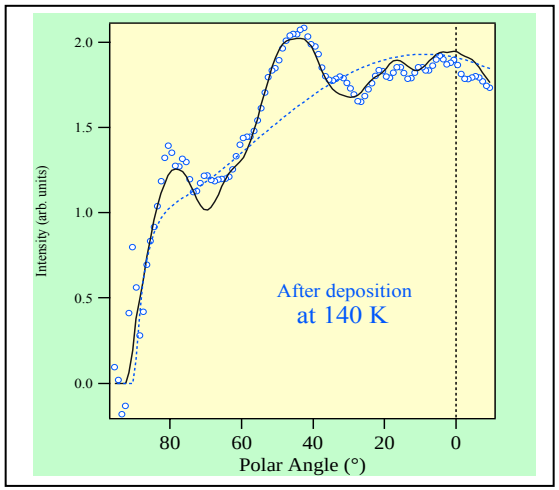


**Trilayer islands**
**Fe-Fe = 1.83 Å**
**Fe-Cu3Au = 1.67 Å**

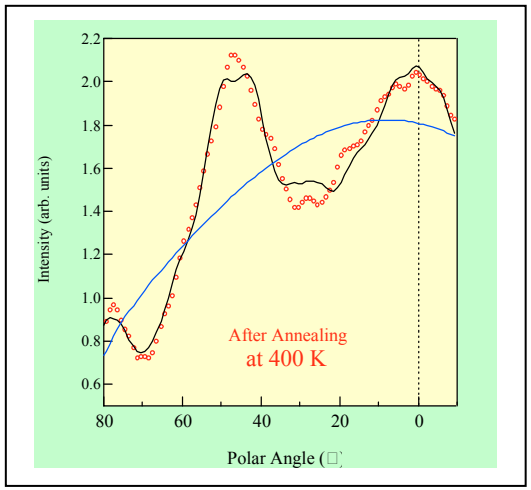

# Check for Au segregation

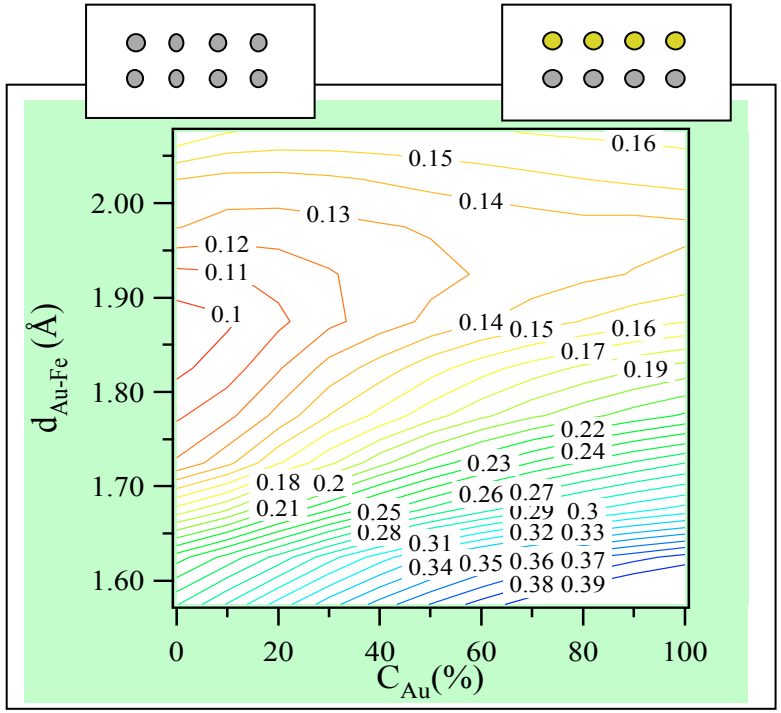


Bilayer islands
No Au segragation

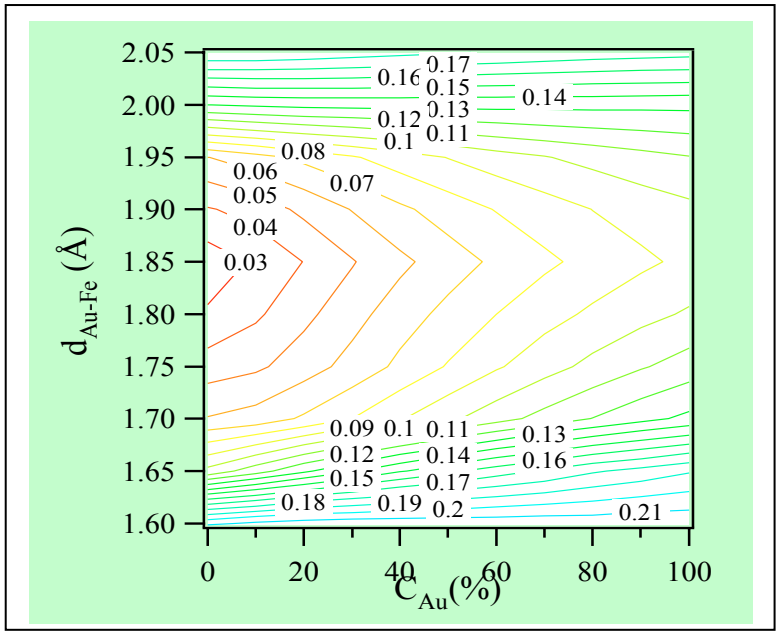


Trilayer islands
No Au segragation

Bilayer islands at 140 K
Absence of Au segregation

⇓

Island morphology driven by electronic effects

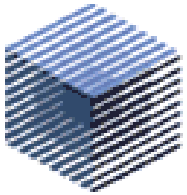

# The pseudomorphic to bulk fcc phase transition of thin Ni films on Pd(100)


**Laboratorio TASC-INFM, Trieste**

**ALOISA beamline staff**

Luca FLOREANO

Albano COSSARO

Francesco BRUNO

Dean CVETKO

Alberto MORGANTE

**Dipartimento di Scienze Chimiche e unità di ricerca INFM, Università di Padova**

GianAndrea RIZZI

Mikhail PETUKHOV

Francesco SEDONA

Gaetano GRANOZZI

# In-situ X-ray Diffraction and Photoemission experiments at the INFM-ALOISA beamline (Trieste)

- In-plane Surface X-ray Diffraction (XRD) to measure the formation of the relaxed **bulk-like phase**.
- Out-of-Plane XRD (ROD scans) to measure the layered structure evolution of the **pseudomorphic phase** during the phase transition.
- X-ray Photoelectron Diffraction (PED) and Spectroscopy (XPS) of the core level shifts and Valence Band to follow the **intermixing at the interface**.
- X-ray Reflectivity (XRR) to measure the perpendicular structure of the **bulk-like phase**.

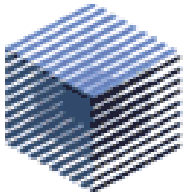

• Both Pd and Ni have a Face Centered Cubic (fcc) structure.

• The **Pd** lattice parameter is **10.5 % larger** than the **Ni** one.

• **Ni grows pseudomorphic to Pd(100)** with a tetragonally strained (fct) structure.

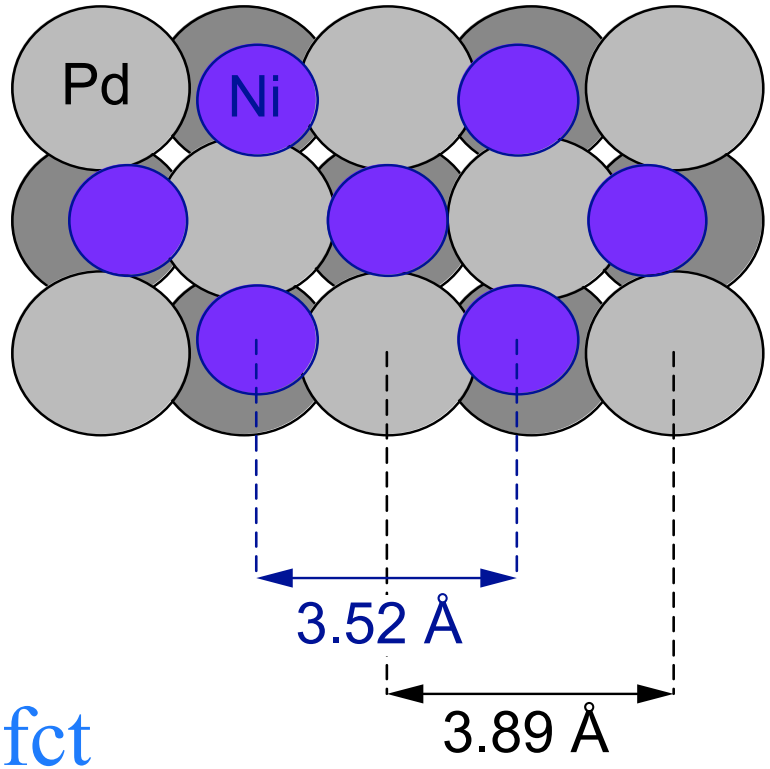


Ni fcc

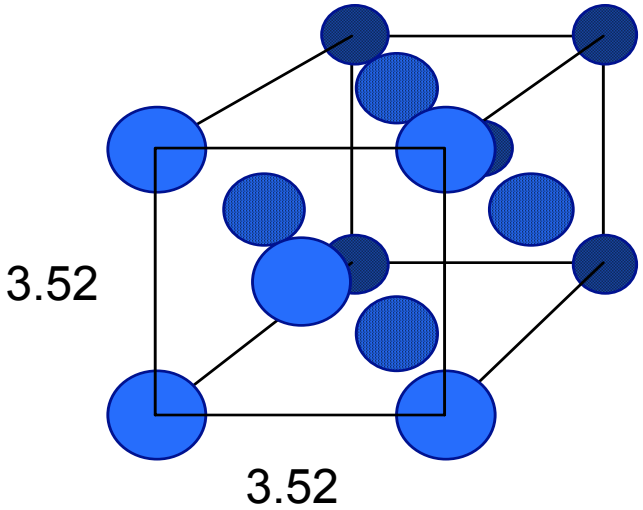


Ni fct

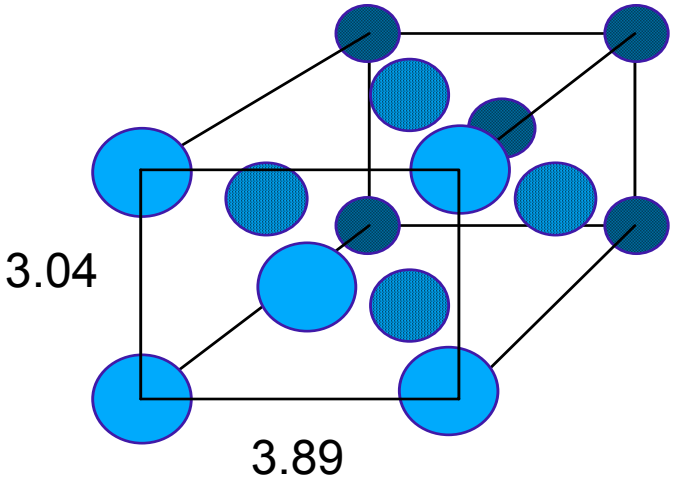


The vertical spacing of the Ni fct structure has been measured to be 1.52 Å.

G.A. Rizzi et al., Surf. Sci. **522** (2003) 1

# In-plane X-ray Diffraction radial scan

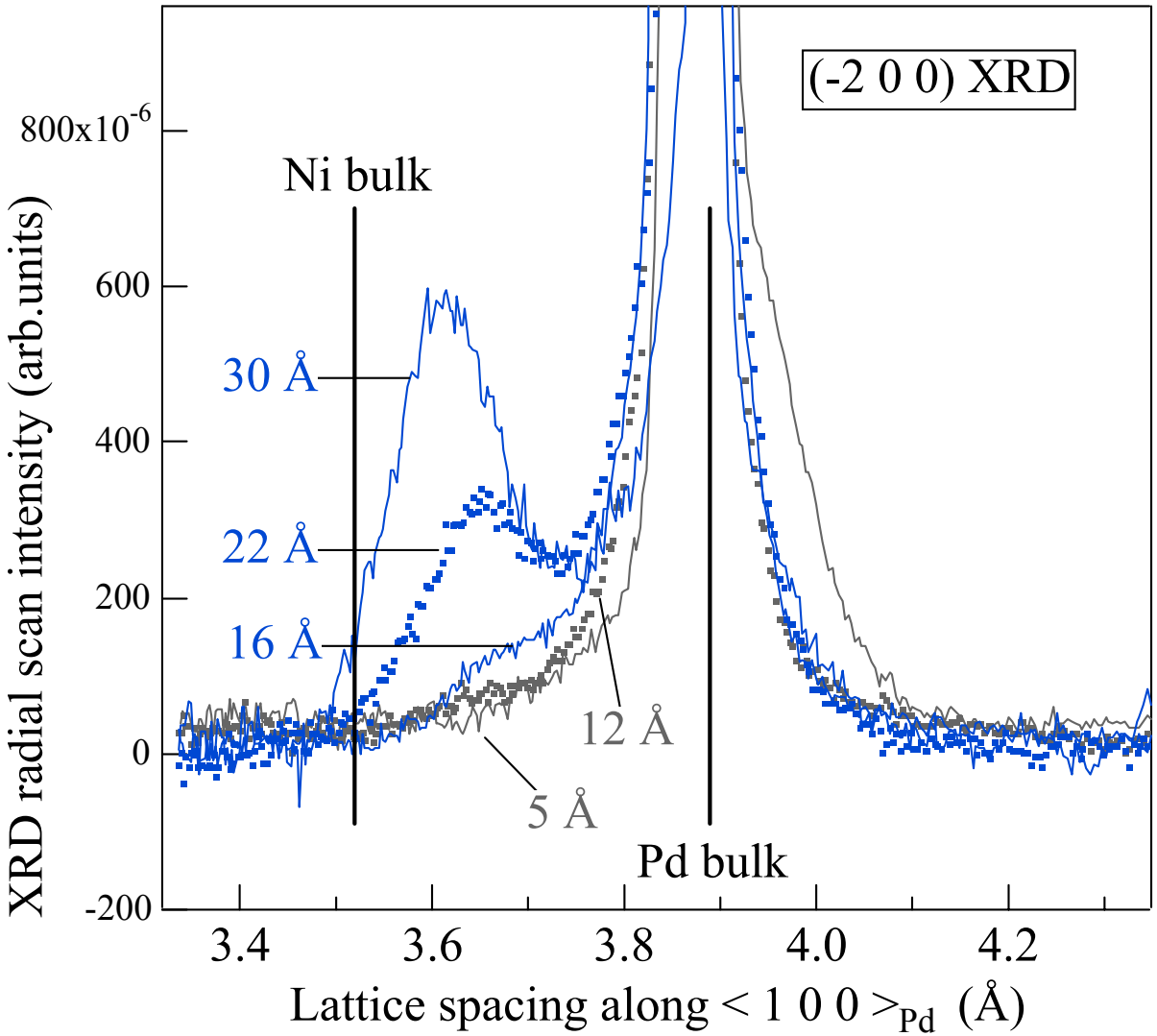


- **Room Temperature** growth
- Ni grows pseudomorphic to Pd(100) up to a 12 Å coverage.
- The appearance of a **shoulder** in the radial scan **at 16 Å** coverage witnesses the formation of a relaxed **bulk-like Ni phase**.
- The new relaxed phase evolves towards the Ni bulk phase as the film thickness increases.

## Out-of-plane XRD, (-2 0 L) ROD scan

• Increase of the number of oscillations from 8 to 12 Å due to increase of the Ni pseudomorphic layers from 6 to 10.

• Decrease of the oscillation amplitude due to the decrease of the sharpness of the interfaces and coverage of the pseudomorphic film.

• No shift of the minima position from 12 to 18 Å ⇓

**no change** of the number of Ni pseudomorphic layers → **limit thickness** for pseudomorphic growth

**Lateral growth of the bulk-like phase domains.**

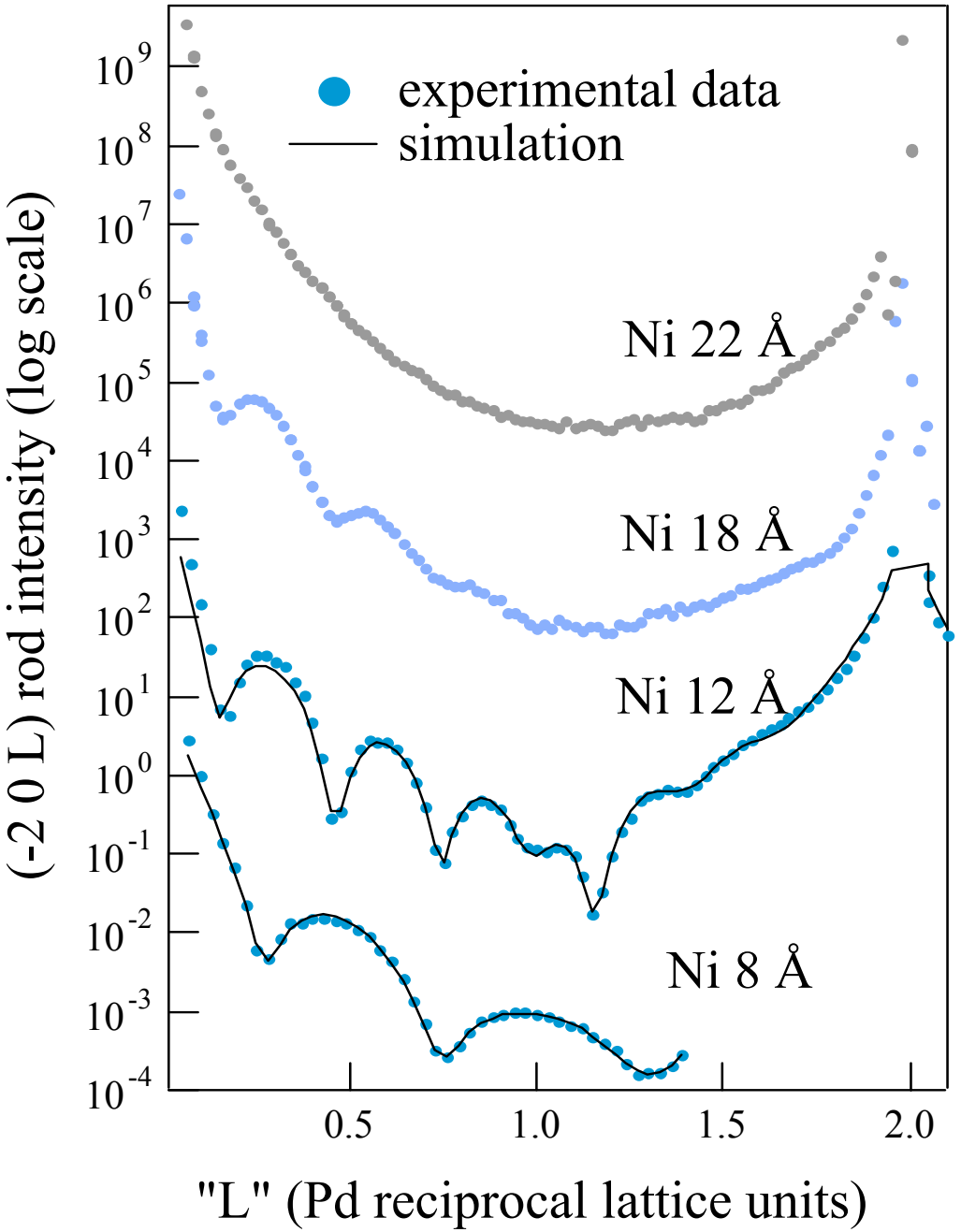

# Structural analysis of pseudomorphic Ni films

The **limit thickness** of stability of the Ni pseudomorphic phase is **10 layers**.

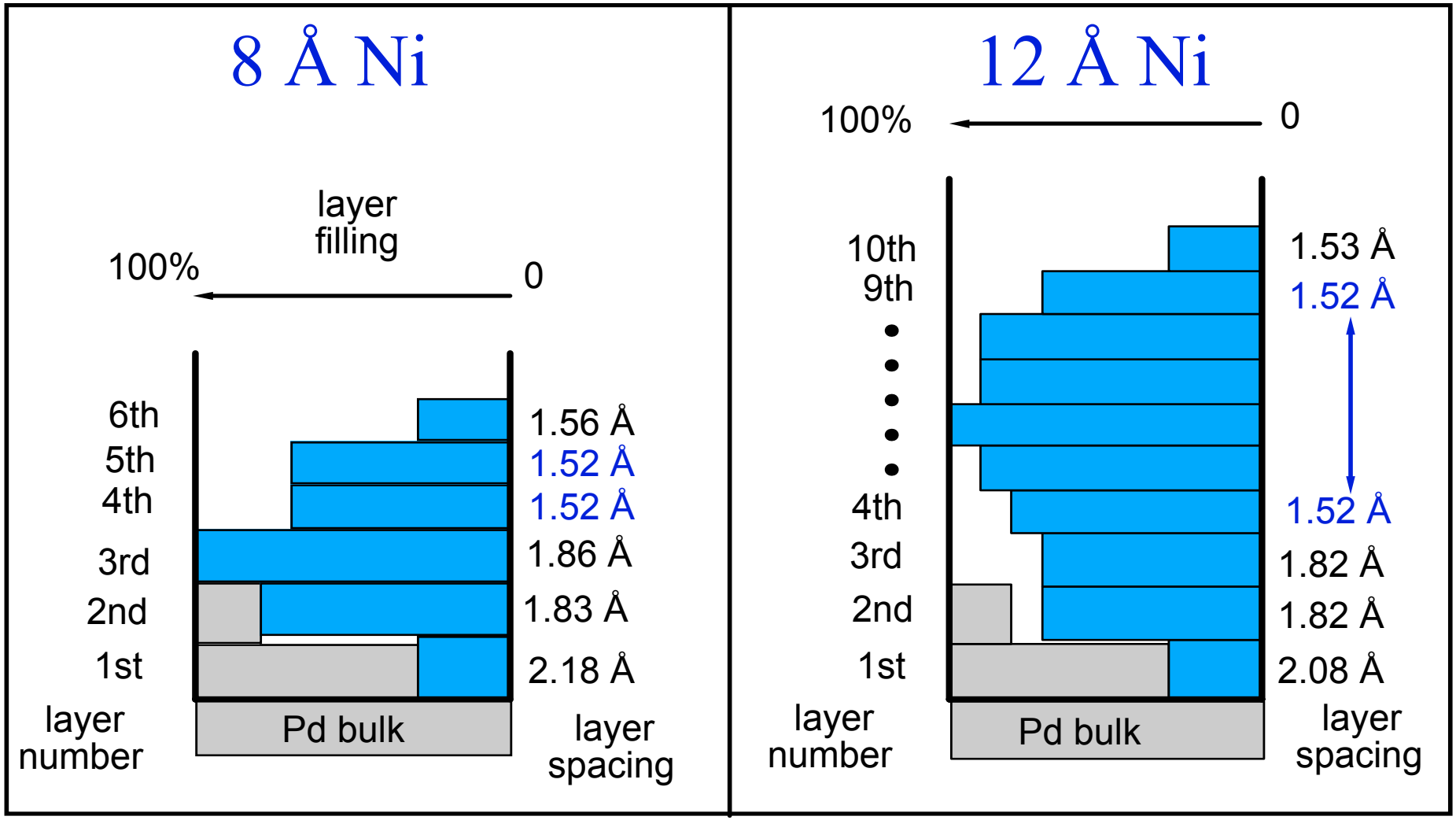

# X-ray Valence Band spectroscopy at 2.5 Å Ni coverage

• The difference spectrum between the 2.5 Å Ni/Pd VB and the clean Pd one displays a peak at B.E.=5 eV (this satellite peak shifts towards the Ni bulk value of 6 eV as the thickness increases) .

• The shift of the Ni VB satellite peak indicates the formation of a **NiPd alloy** (in agreement with the observed Pd 3d core level shift).

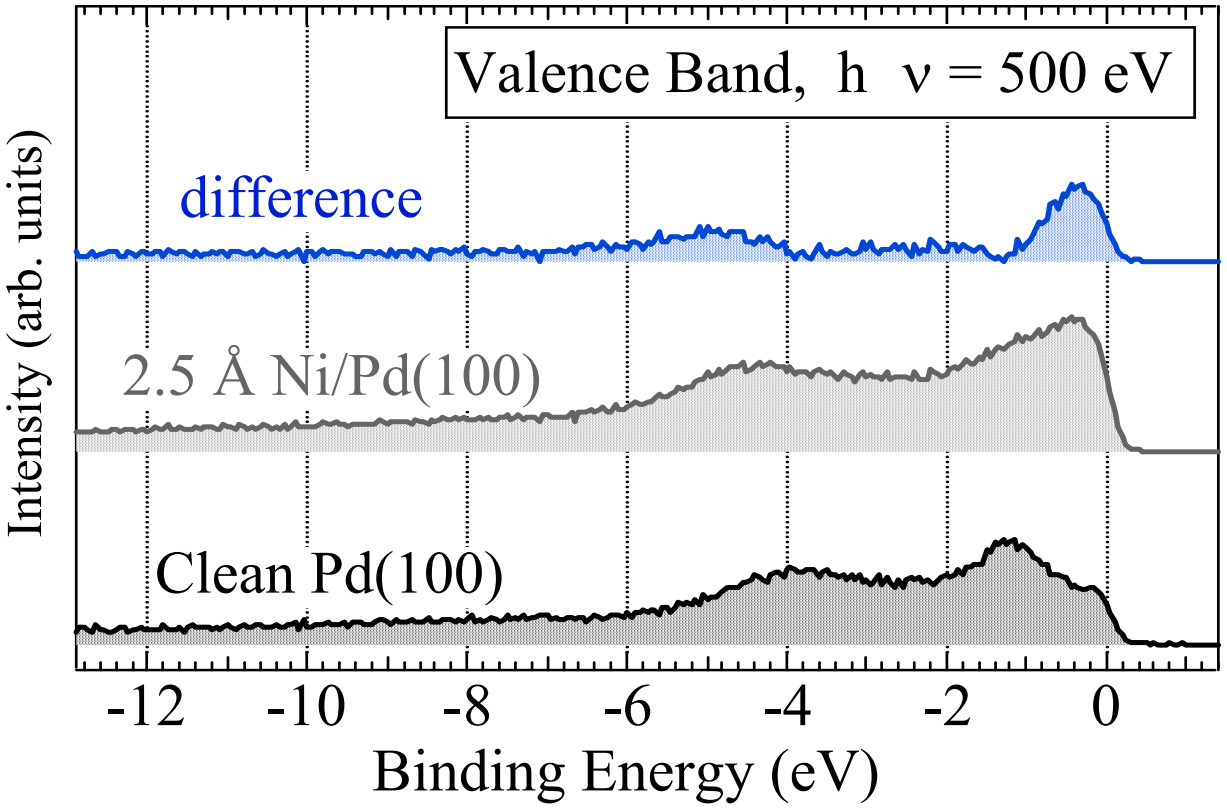

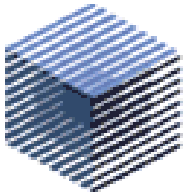

# X-ray Photoelectron Diffraction of Ni 2p core level

- **Enhanced pseudomorphism** of the **2.5 Å film**, probably due to intermixing (cfr. RODs, XPS, VB).
- At 2.5 Å, a weak peak along the surface normal (due to 3rd layer atoms) indicates both roughness and intermixing.
- Due to elasticity laws, a vertical compression of the pseudomorphic phase sets in at 5 Å.
- **The strain** of the pseudomorphic Ni phase **is released at a critical coverage of 16 Å** (cfr. XRD radial scans).

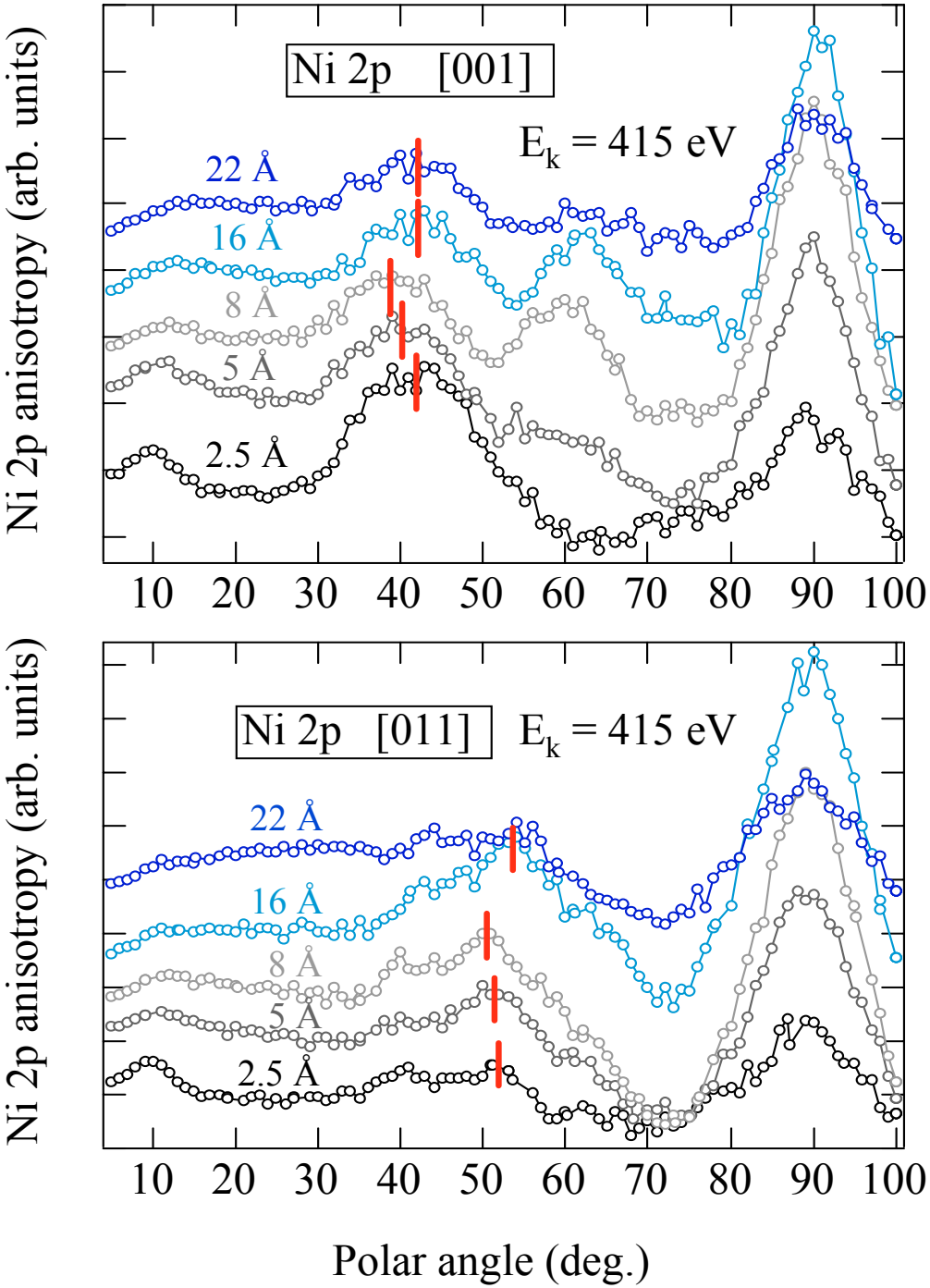

# X-ray Photoemission of Pd 3d core level

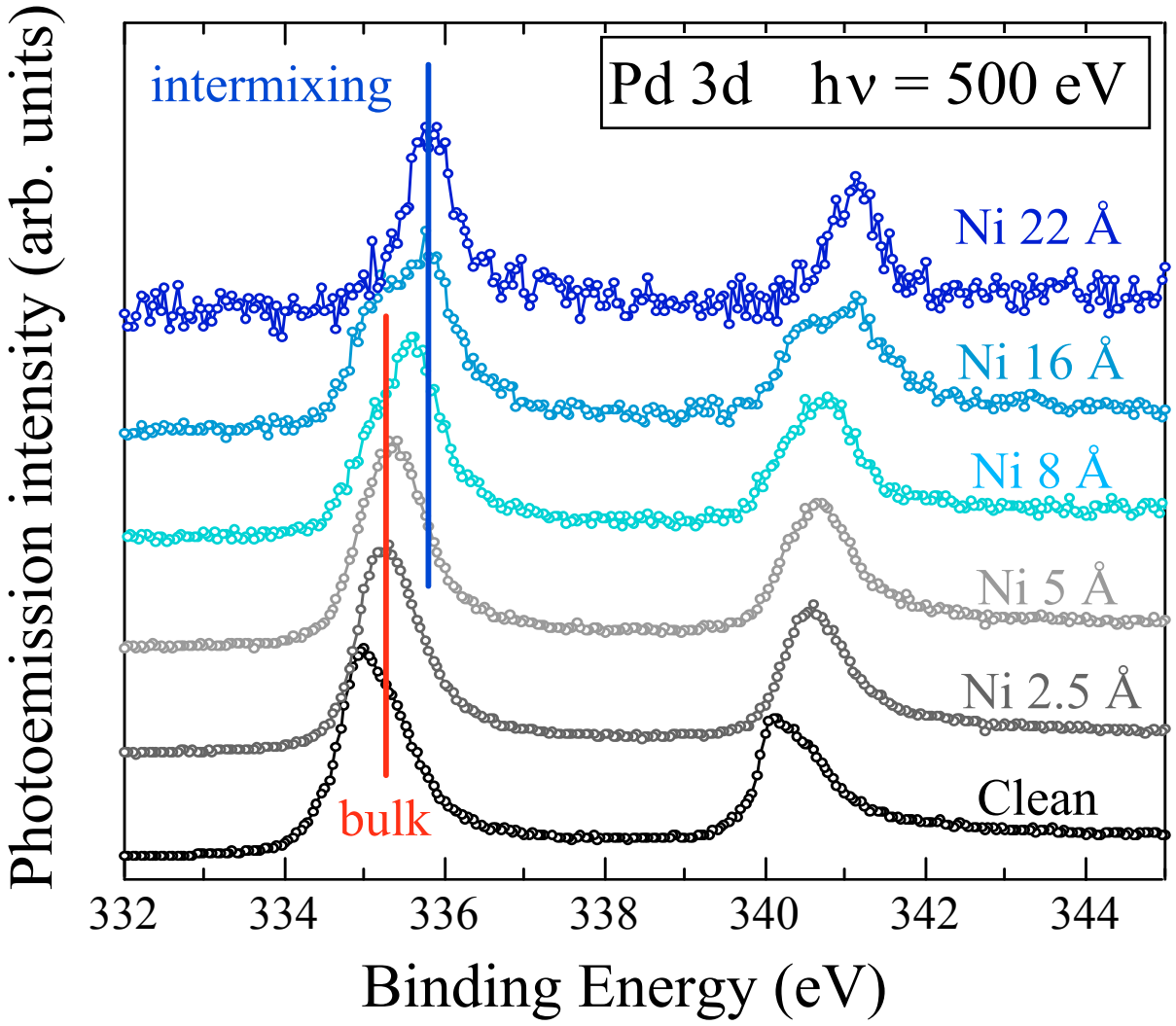


- Pd $3d_{5/2}$ from the clean substrate displays a bulk component at B.E.=335.2 eV and a surface component at ΔE=-0.35 eV.
- The surface component is replaced by **a new component** (ΔE=+0.65 eV) upon Ni deposition, which **becomes dominant at a 16 Å coverage.**
- The new component is **assigned to Pd/Ni alloying** from comparison with Valence Band spectroscopy.
- The Pd 3d signal disappears beyond a coverage of 22 Å.

# XPS analysis of Pd 3d core level shifts

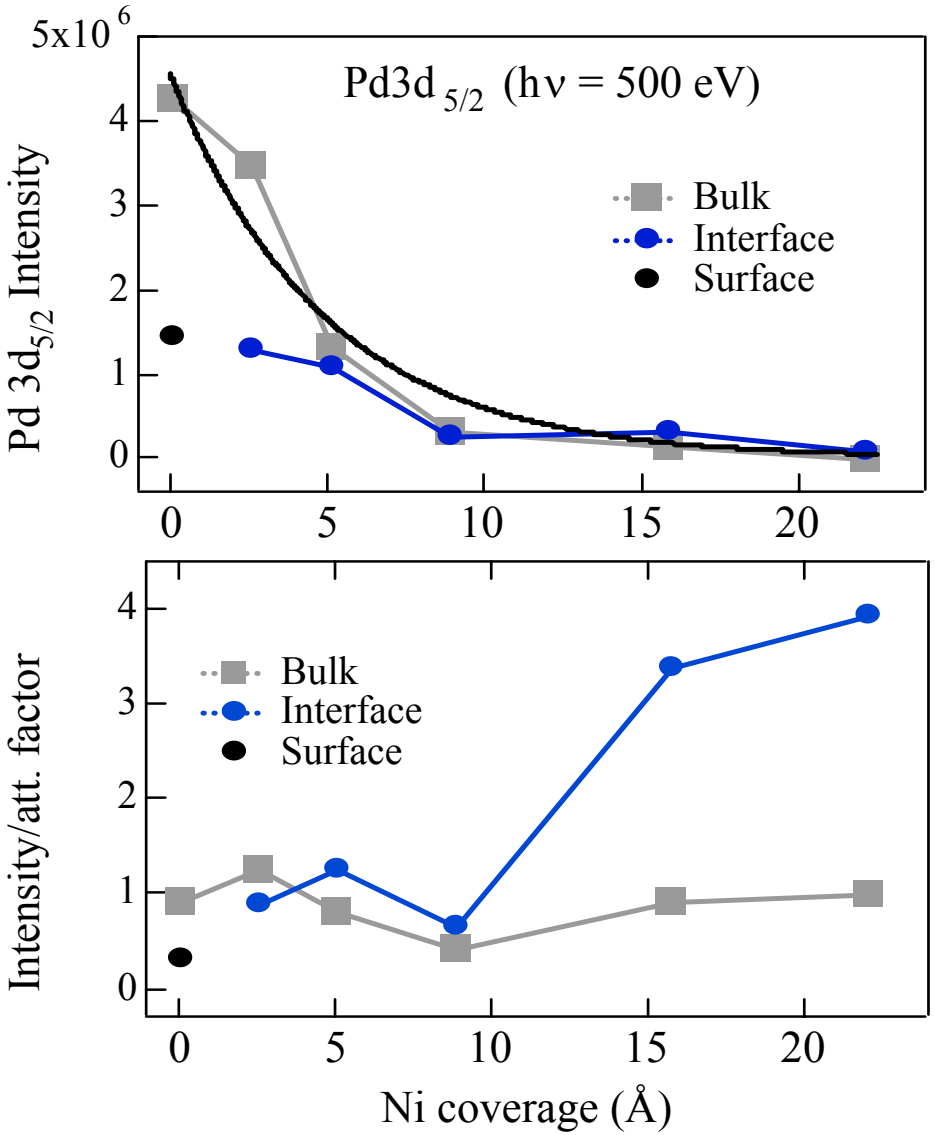


• The intensity of the Pd 3d **bulk component follows a regular exponential decay** as a function of the overlayer Ni coverage → **no dewetting** beyond the transition.

• A different decay law is observed for the alloying component.

• Normalization to the bulk exponential decay highlights the behavior of the interface component.

• **Alloying suddenly increases at the critical coverage of 16 Å**, where the film transforms into the bulk-like phase.

• The Pd 3d signal fully disappears below a 30 Å Ni film, i.e. the alloying component is not due to segregated Pd, but to intermixing at the Ni/Pd interface.

# X-ray Reflectivity of the bulk-like Ni phase

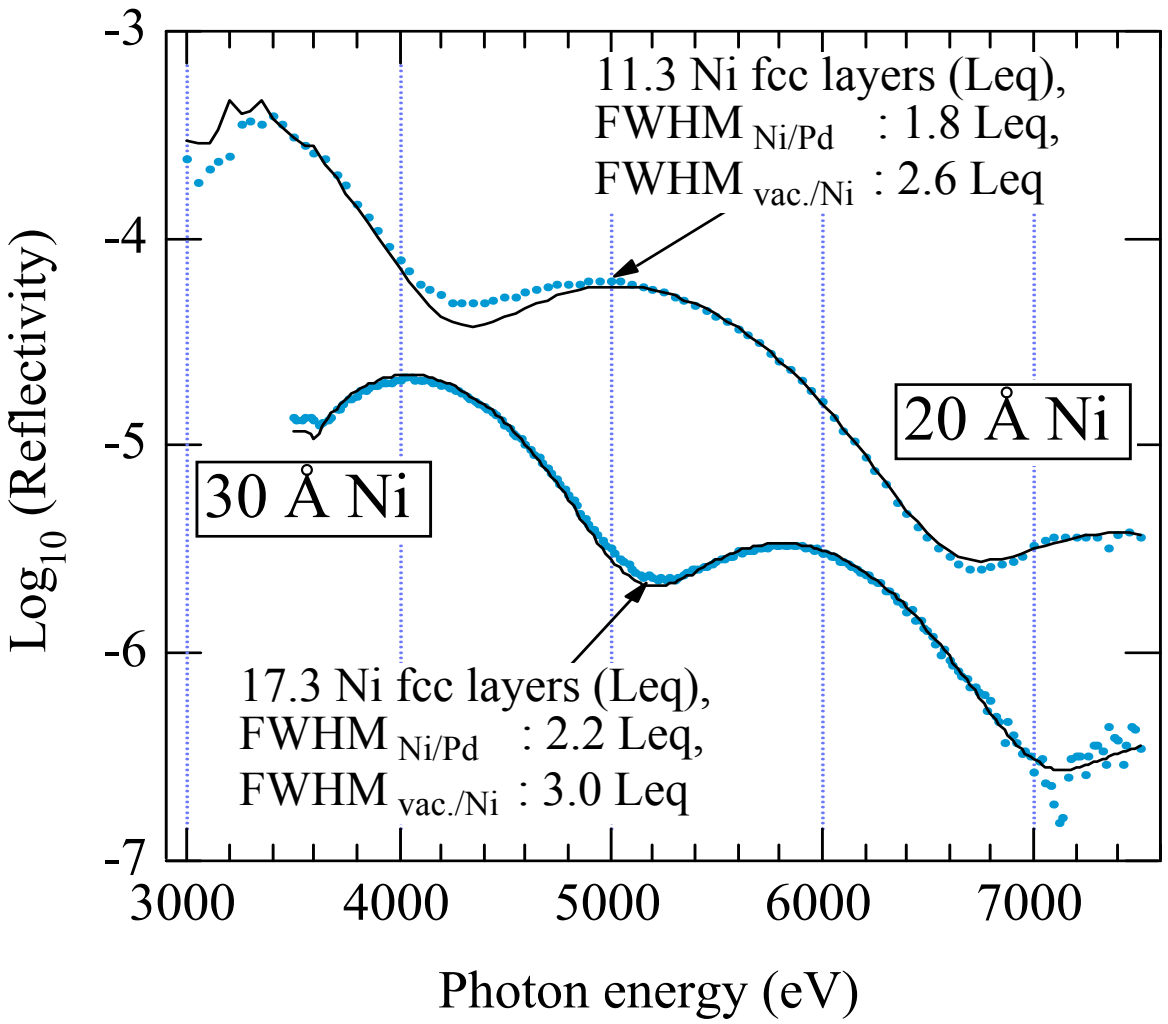


• Perpendicular momentum scan of the specular reflectivity by photon energy scan at fixed scattering geometry.

• **Fitting to a Ni fcc bulk model** (layer spacing of 1.76 Å).

• The fit quality is lower for the 20 Å film due to large residual strain of the Ni bulk-like phase.

• The **relative surface roughness remains about 20 %** of the film thickness.

⇓

**NO dewetting** (2D→ 3D)

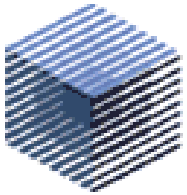

# Ni film evolution

• **1 - 3 Å** : fully pseudomorphic Ni film, partially intermixed with Pd.

• **4 - 12 Å** : tetragonally strained pseudomorphic structure, the Ni lattice cell is vertically compressed according to elasticity laws. The Ni film is fully wetting the substrate. No change of intermixing at the interface.

• **12 Å** : the Ni film achieves the limit thickness of stability of the pseudomorphic phase, corresponding to 10 layers (some of them partially intermixed or partially filled).

• **15 - 18 Å** : critical coverage for the onset of the structural transition. Coexistence of pseudomorphic fct and bulk-like fcc phases. Increase of Ni/Pd intermixing together with the appearance of a LEED Moirè pattern [decoration spots with (10x10) periodicity, in agreement with the 10% lattice mismatch].

• **> 18 Å** : the bulk-like phase evolves towards the bulk fcc structure by a gradual release of the reidual strain. The bulk-like phase is still fully wetting the substrate.

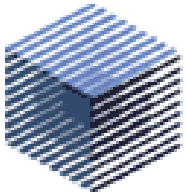

# Conclusions

- The fcc domains grow by lateral propagation of the domain walls while the residual fct domains preserve their thickness and layered structure.
- The fct $\rightarrow$ fcc phase transitions is driven by defects (domain walls) propagating from the interface to the surface of the Ni film.
- LEED patterns suggest the domain walls to be shear planes in the <110> direction.
- The limited roughness across the critical coverage of 16 Å excludes a dewetting (2D $\rightarrow$ 3D) transition .
- The fct $\rightarrow$ fcc phase transition is of the martensitic type (1st order, non-diffusive transition).

# Structure of Methylthiolates on the Au(111) Surface

Self Assembled Monolayers (SAMs) of thiols on gold are prototypical metal-organic junctions of ubiquitous application in nanoscience

- Molecular electronic devices
- Surface Coatings
- Nanolithography
- Biosensors

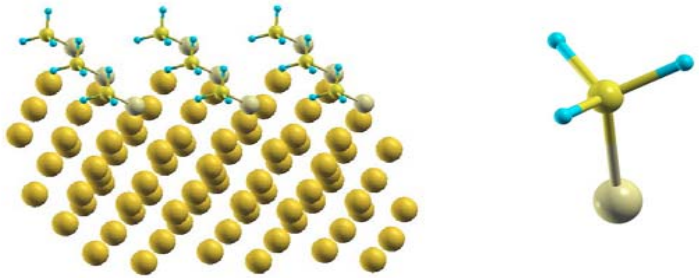

The metal-organic interaction is not well understood and even the structure of the simplest of these materials ($Au(111)SCH_3$) is under dispute.

- Theory (structural optimization, static structures)

**bridge site**

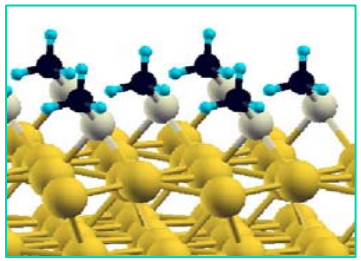

- Experiments - Photoelectron Diffraction, NIXSW (Kondoh, PRL,2003, Roper, Chem.Phys.Lett.,2004)

**on-top site**

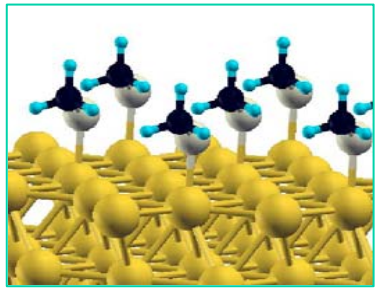

# Photoelectron diffraction

- Normal-emission, energy-resolved data exhibit oscillations with a single period, which are characteristic of a 180 degrees scattering from a near neighbor.

T=200 K

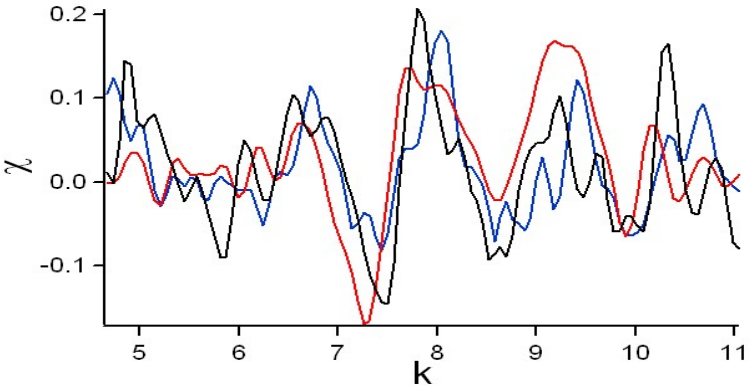


exp
on-top
adatom

S-Au bond ~ 2.5 Å

- Angle-resolved PED (k=4.6)

exp

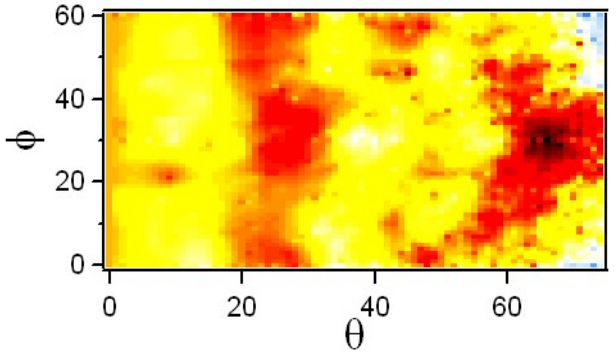


adatom

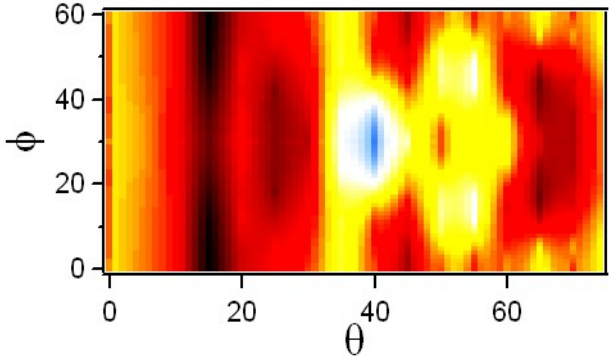


on-top

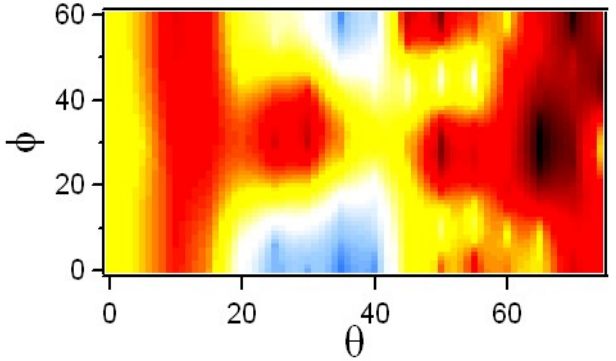


MSCD (http://www.sitp.lbl.gov/mscdpack/mscdpack.html)

# X-Ray Diffraction

T=200K

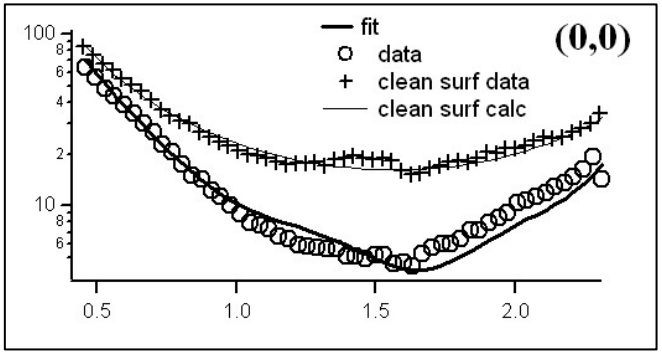


- reflectivity results: pronounced drop in intensities for large $q_z$ not accounted for by a flat, defect-free Au surface
- disordered structure: 1° layer Au atoms modeled by multiple sites with fractional occupancies
- variable occupancies associated with adatoms and vacancies (adatom population 0.3)

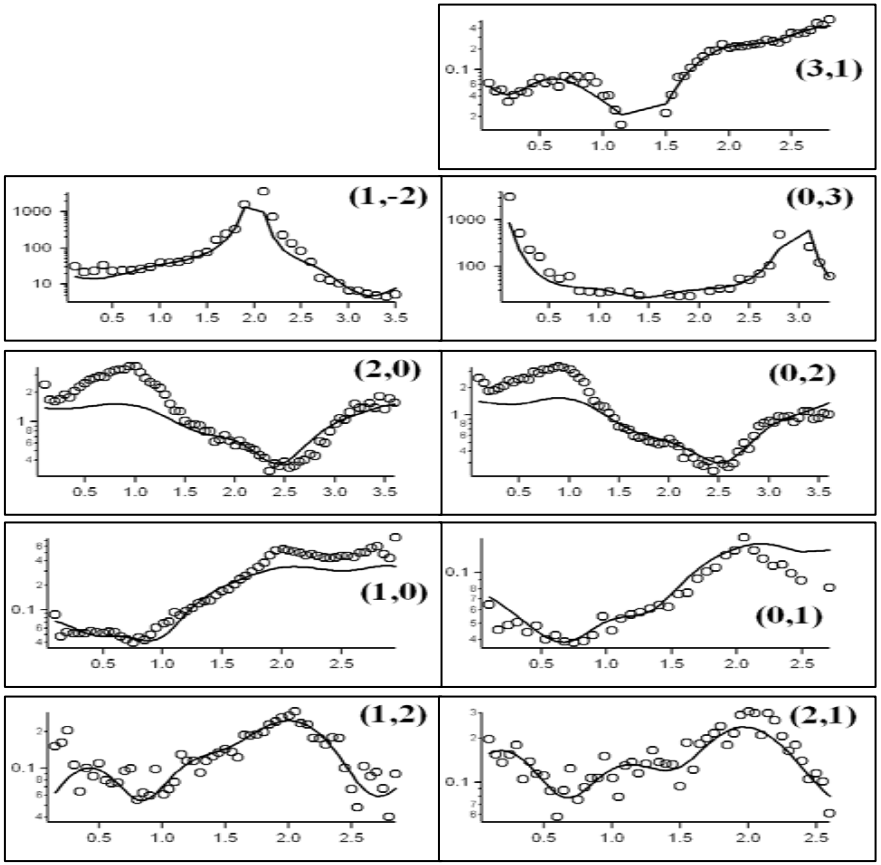


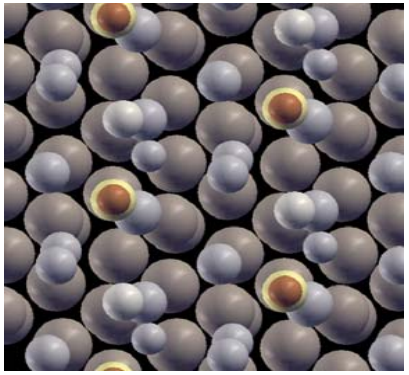

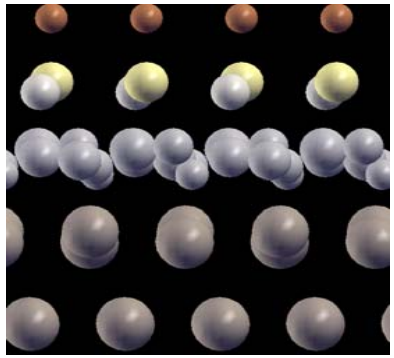

# Molecular Dynamics

- The formation of on-top sites (as signaled by the breaking of a Au-S bond) is dynamic.
- "Pull-out" mechanism:

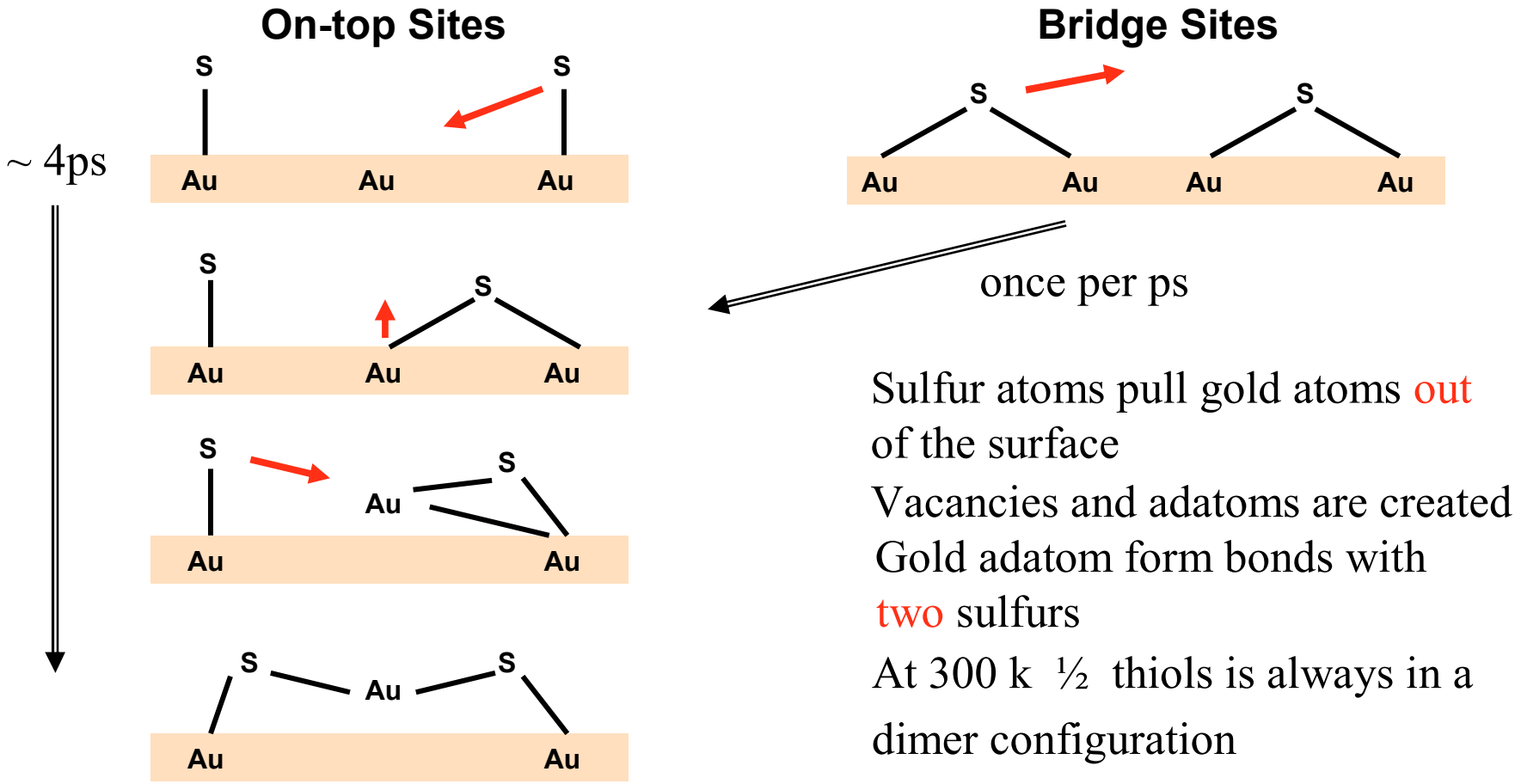


Sulfur atoms pull gold atoms out of the surface

Vacancies and adatoms are created

Gold adatom form bonds with two sulfurs

At 300 k ½ thiols is always in a dimer configuration

# L-Cysteine adsorption on Au(110)

Simple aminoacid, model system for adsorption to compare with simpler S bound organic molecules (alkenthiols).

Can be used to bind other more complex organic molecules li proteins, DNA

Complex system for structural determination, molecule with MANY degrees of freedom

Possible formation of intermolecular bonds.

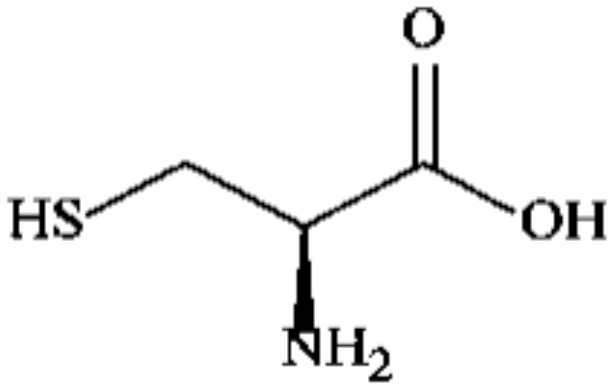


Combination of spectroscopic and structural techniques
Au(110) $\Rightarrow$ anisotropy in the molecular self assembly process.
Molecular beam source for UHV deposition
Spectroscopic studies on L-Cysteine from solution and UHV evaporation on Au(111)
O.Cavalleri et al Phys. Chem. Chem. Phys. 6 2004 4042, J. Phys. Cond. Matter 16 2004, S2477, G. Gonella J. Phys. Chem. B 109 (2005) 18003
Cu-phtalocyanine, pentacene induce restructuring 1x2 Au(110) reconstruction

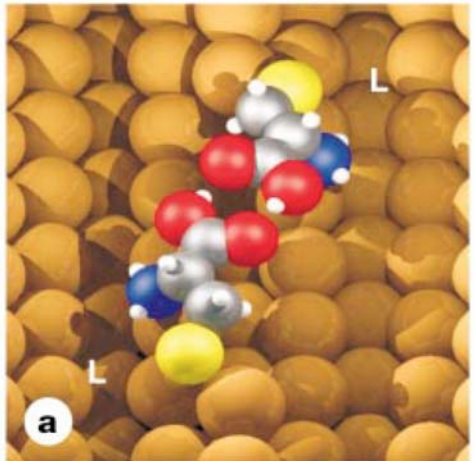


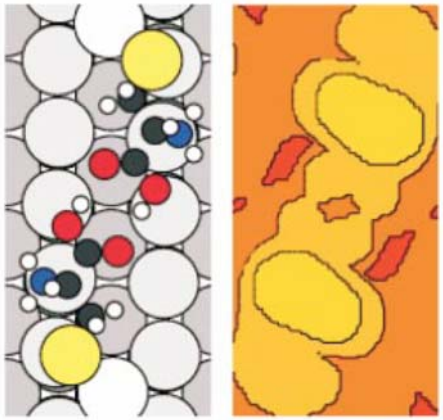

Recent STM and DF theoretical results on L-Cysteine on Au(110)

Chiral recognition of Cysteine dimers at low coverages

Kühnle et al Nature 415 (2002)891

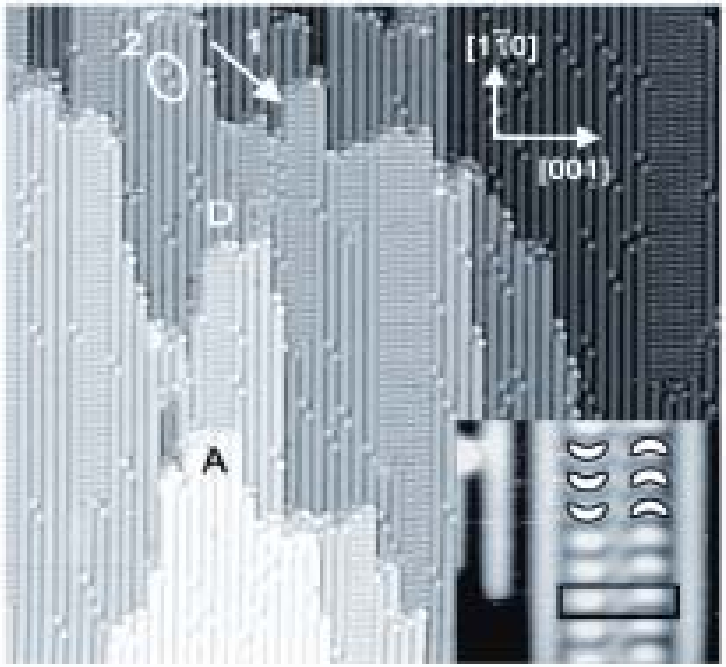


FIG. 1. Large-scale STM image showing coexisting molec
lar structures of D-cysteine on a Au(110)-(1 × 2) surface (425

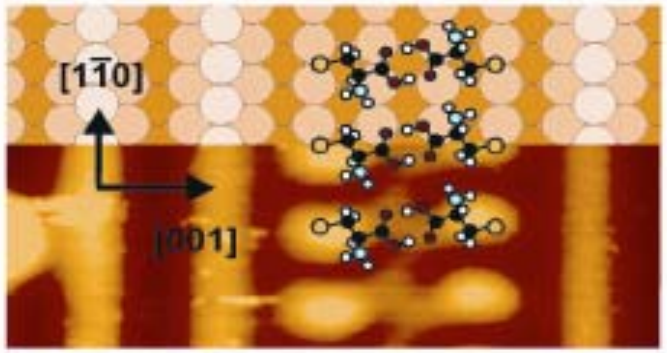


FIG. 3 (color). Most stable cysteine double-row structure, as
obtained from the DFT calculations, superimposed onto an

Formation of molecular rows at higher coverages, restructuring of substrate, long range order?

Kühnle et al. PRL 93 (2004) 86101

# In plane X-ray diffraction: domains size

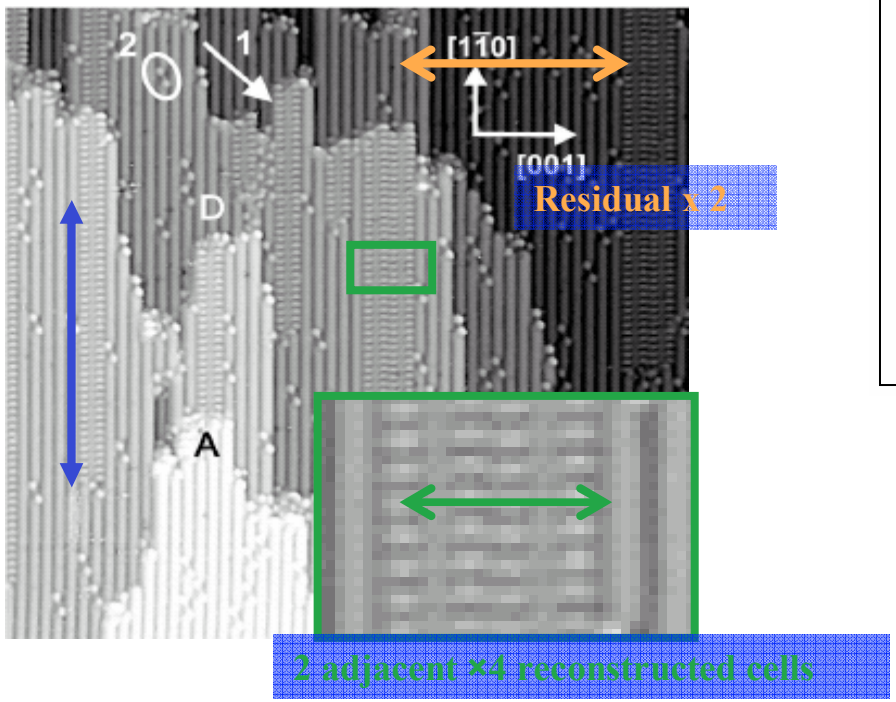


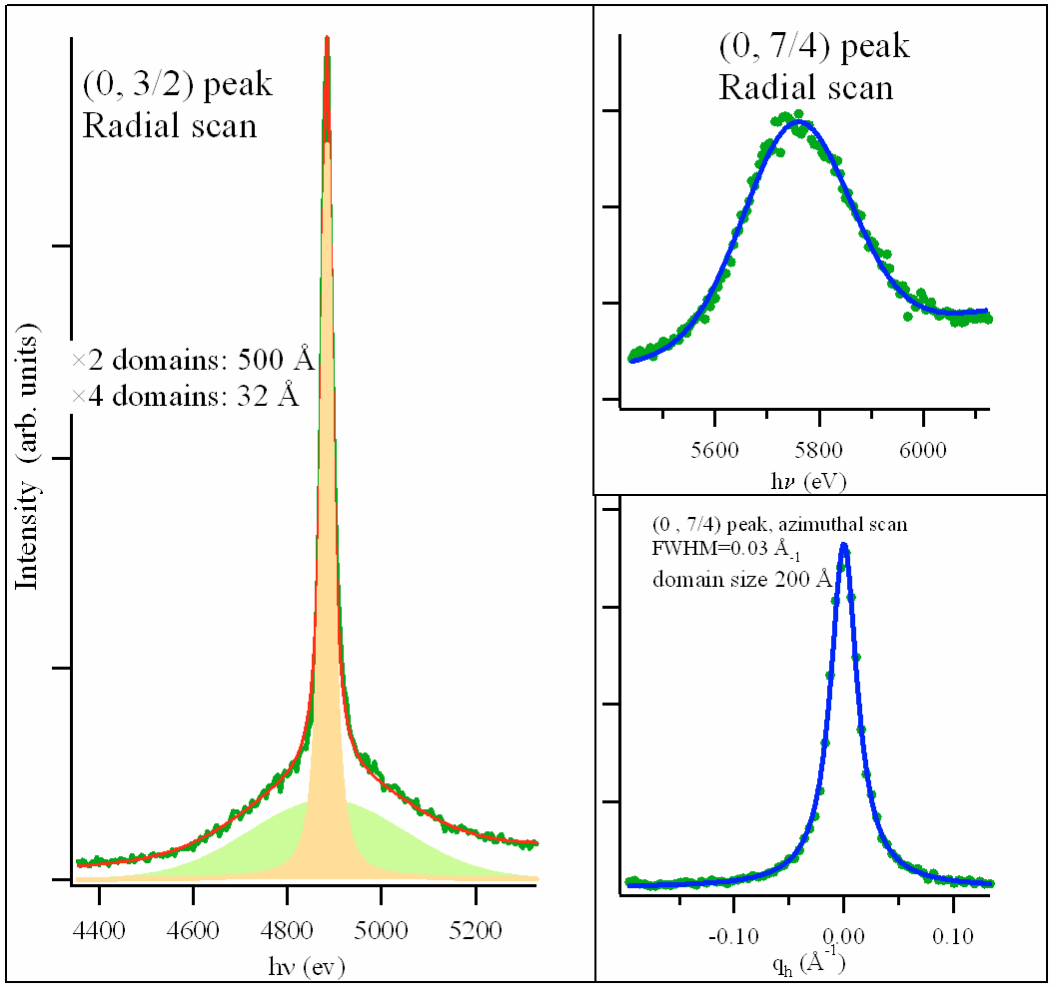


Strongly asymmetric domain size, consistent with STM picture

# The fitting model

**× 4 reconstructed surface** **+** **× 2 missing row clean surface**

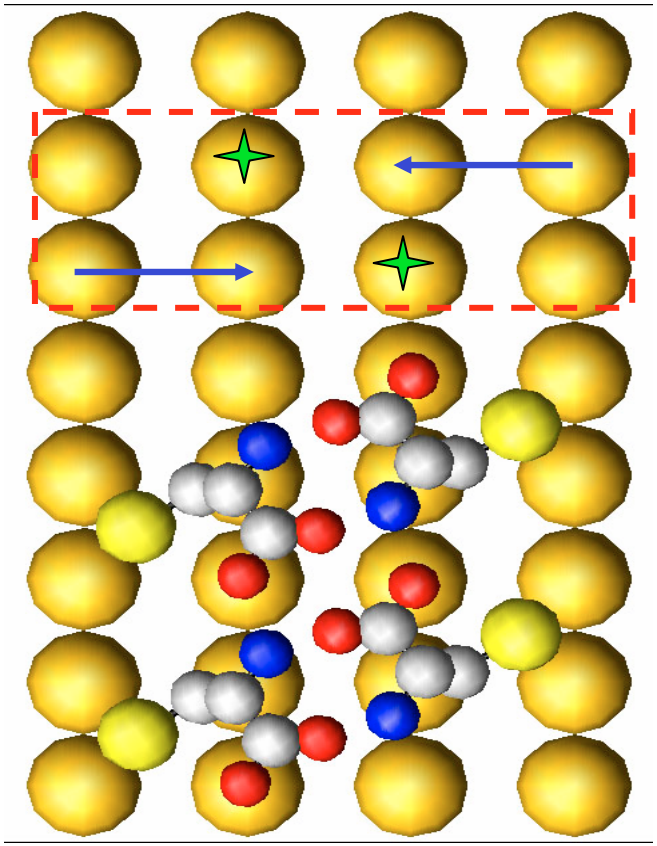

Anti-symmetrical displacements in the unit cell

Two laying down molecules per unit c

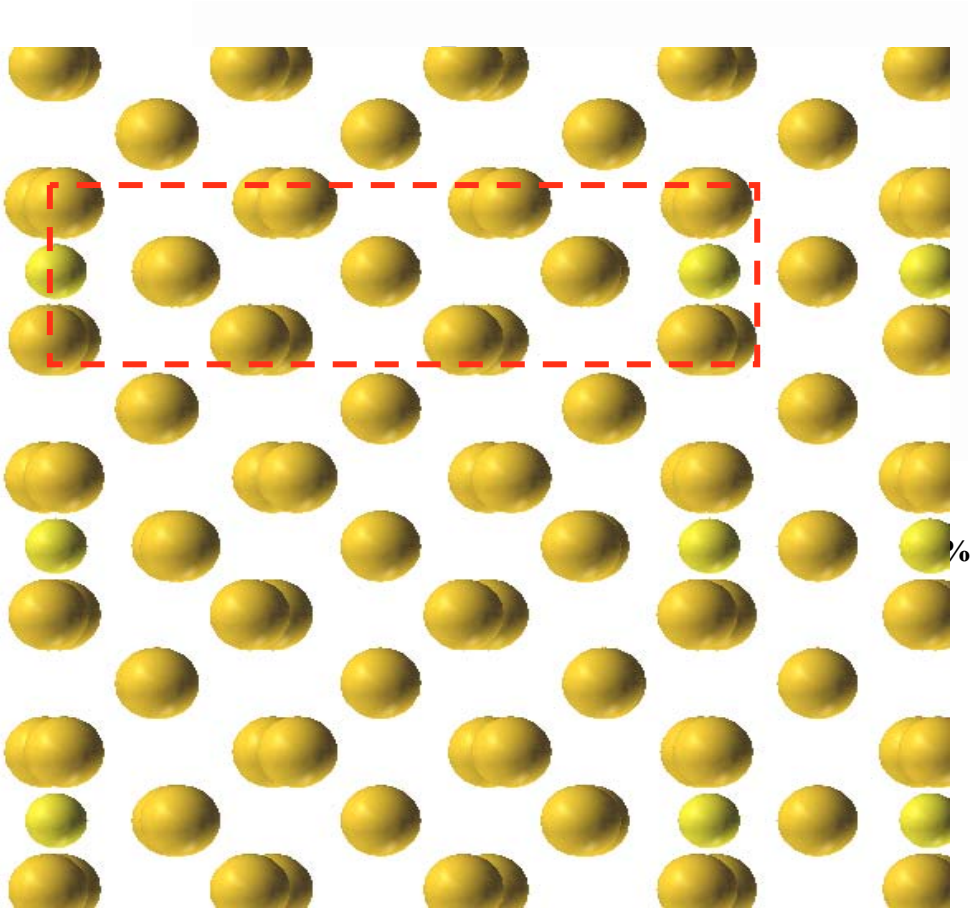

80% ← best fit conditions → 20%

# Out of plane XRD measurements

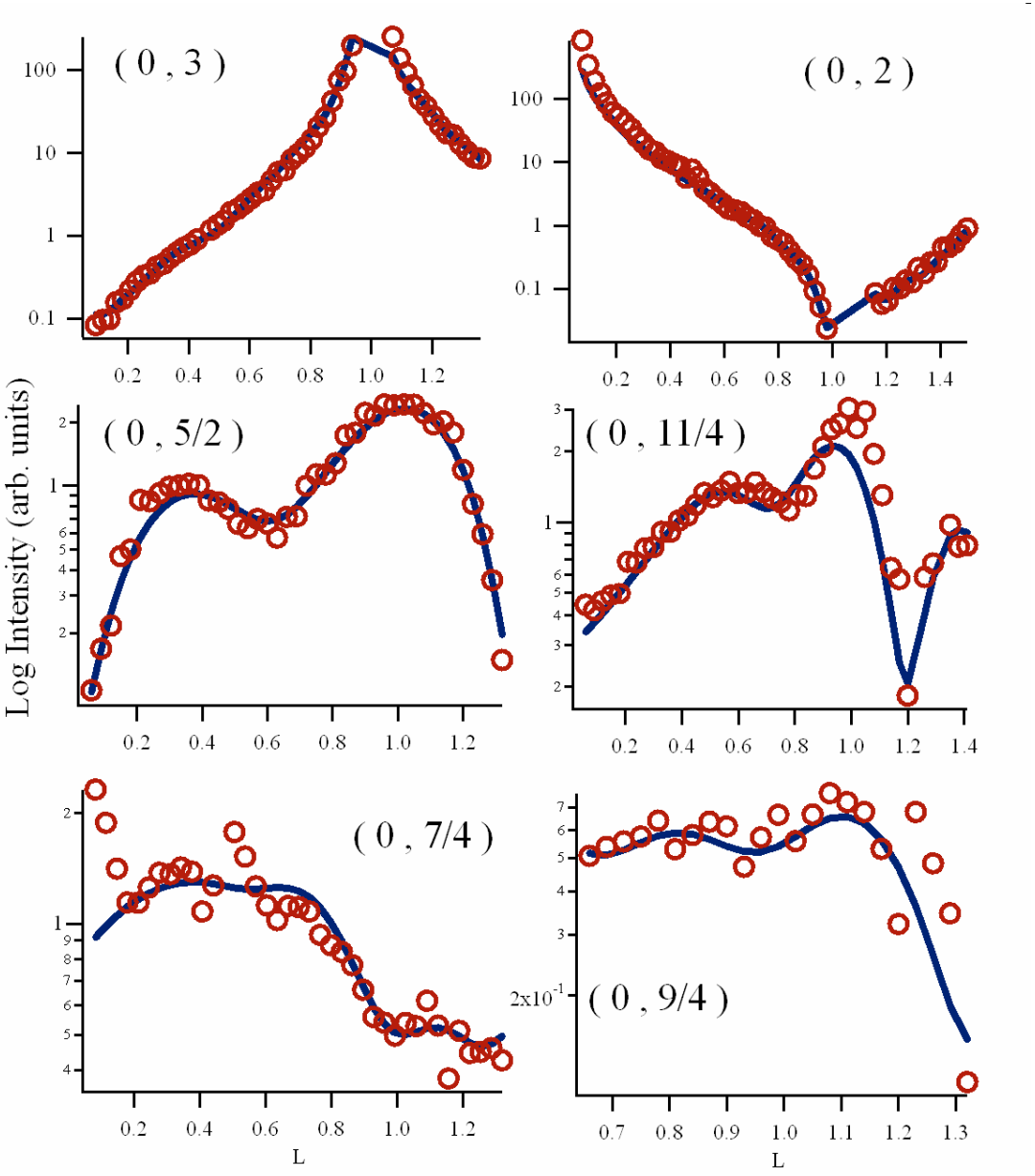


more than 5 Au layers involved

poor sensitivity to the molecules

NEXAFS

# NEXAFS analysis

NEXAFS spectra calculation by Plashkevych et al. Chemical Physics 232 (1998) 49

Calculation for isolated molecule

C1 and C2 contribution can not be resolved for isolated molecules.

C3 Π* contribution

Experimental spectra on L-cysteine powder display similar behavior

Cysteine chemisorption ⇒ C2 atom interacts strongly with substrate ⇒ C2 contribution shifts strongly.

Our high resolution spectra ⇒ Tentative peak association

P1 ⇒ C2 σ* state strong shift due to substrate interaction

P2 FL step? P3 ?

Π* mostly localized on COO group.

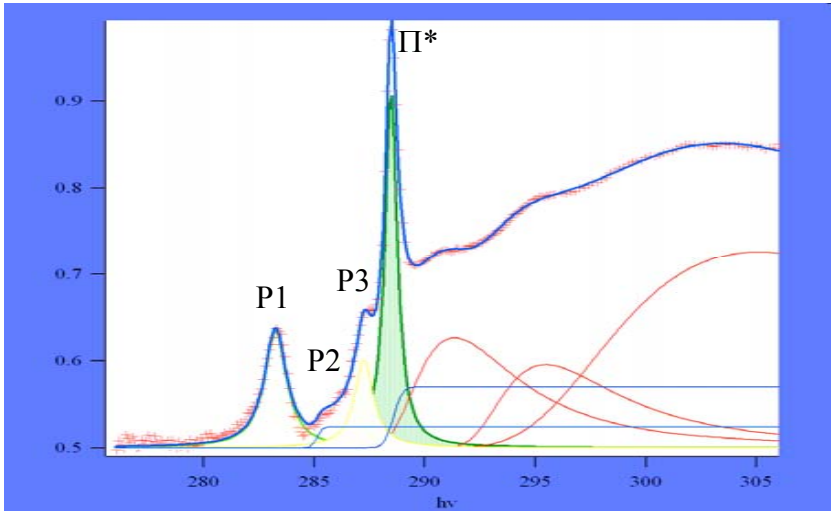


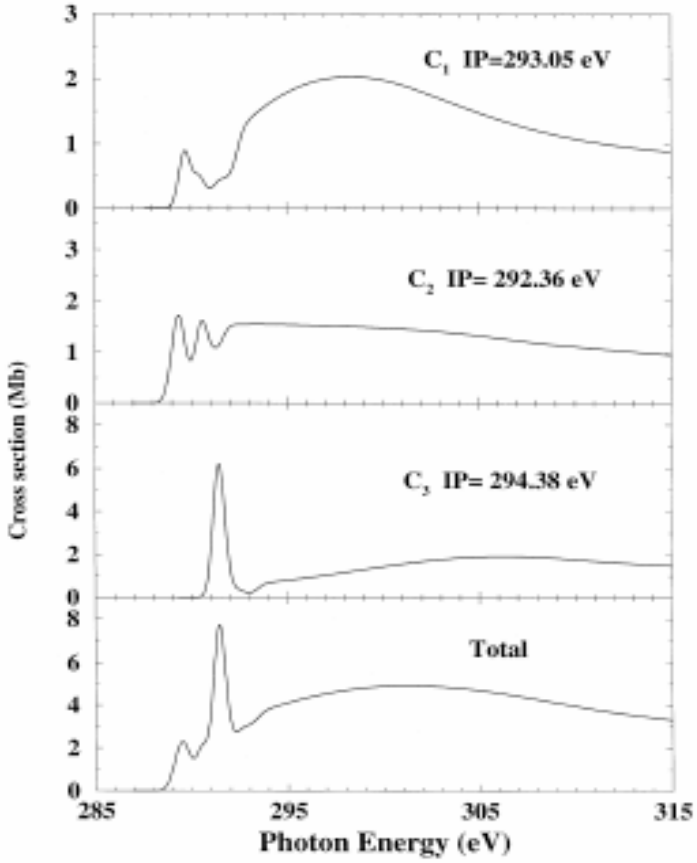


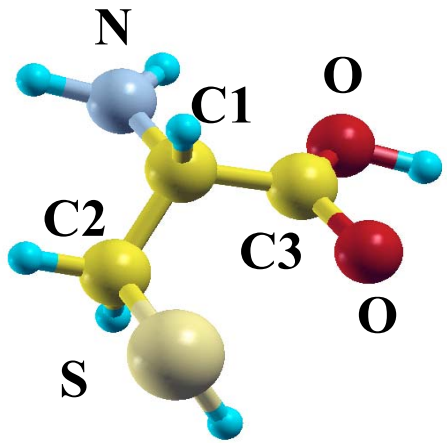

# NEXAFS C1s: azimuthal dependence

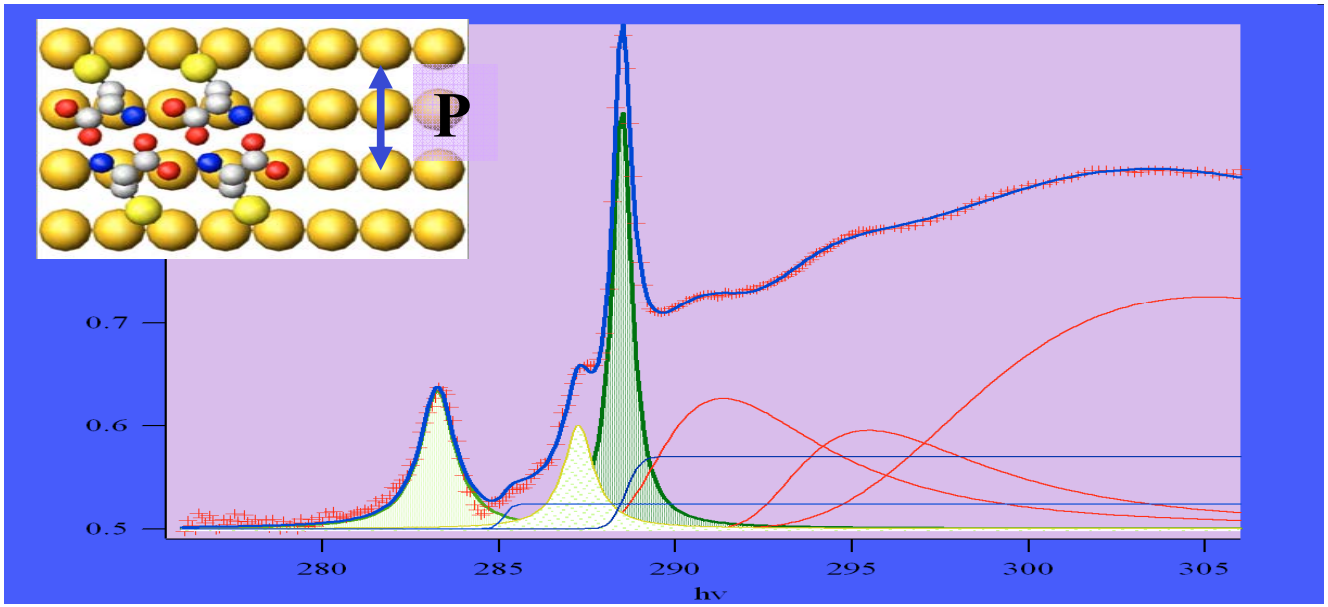


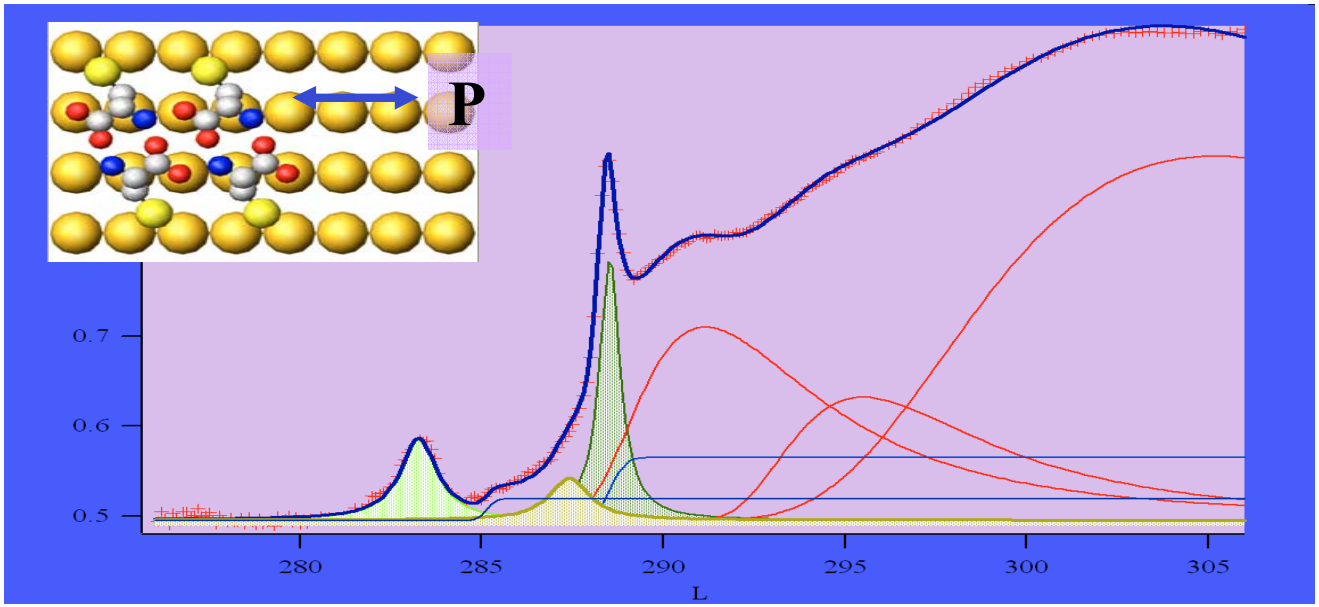

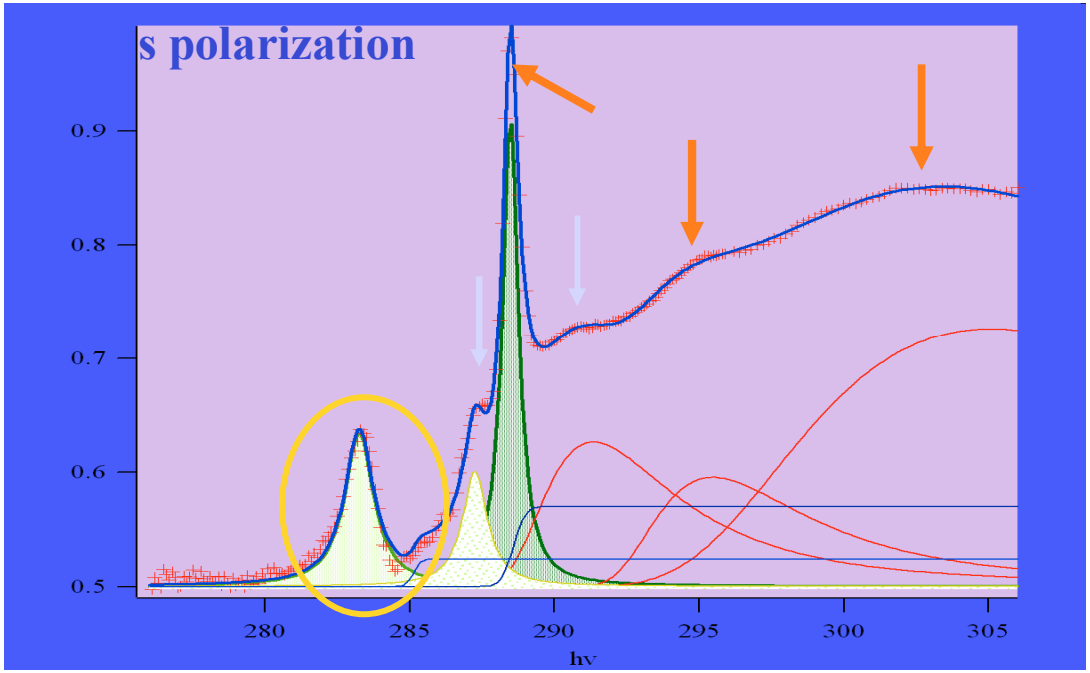


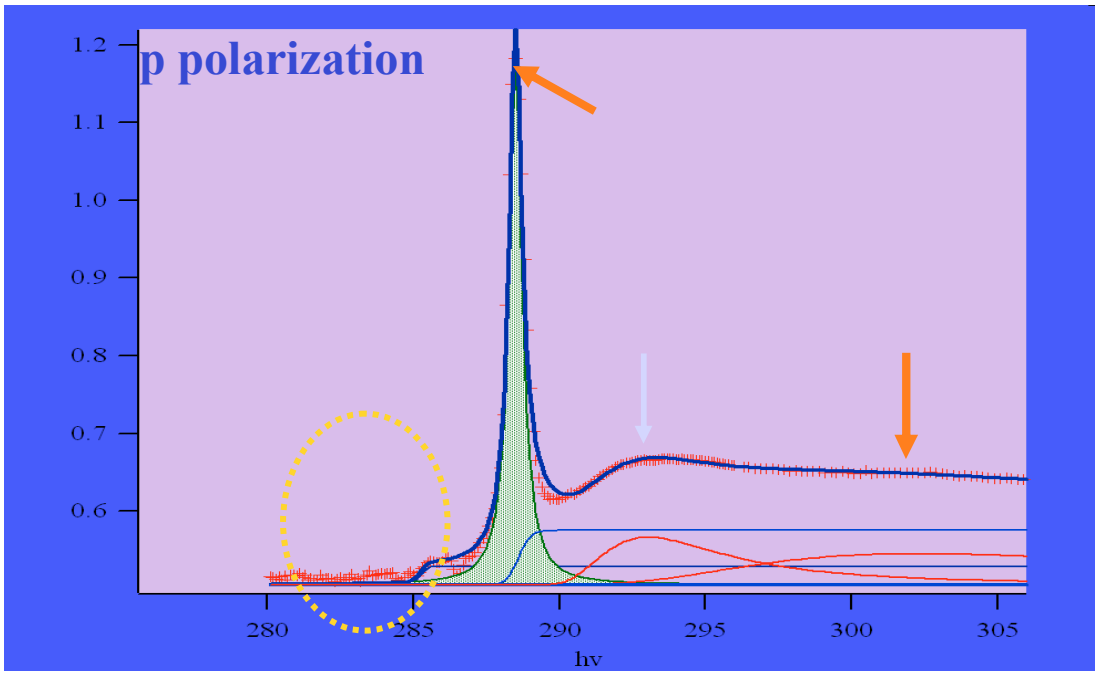


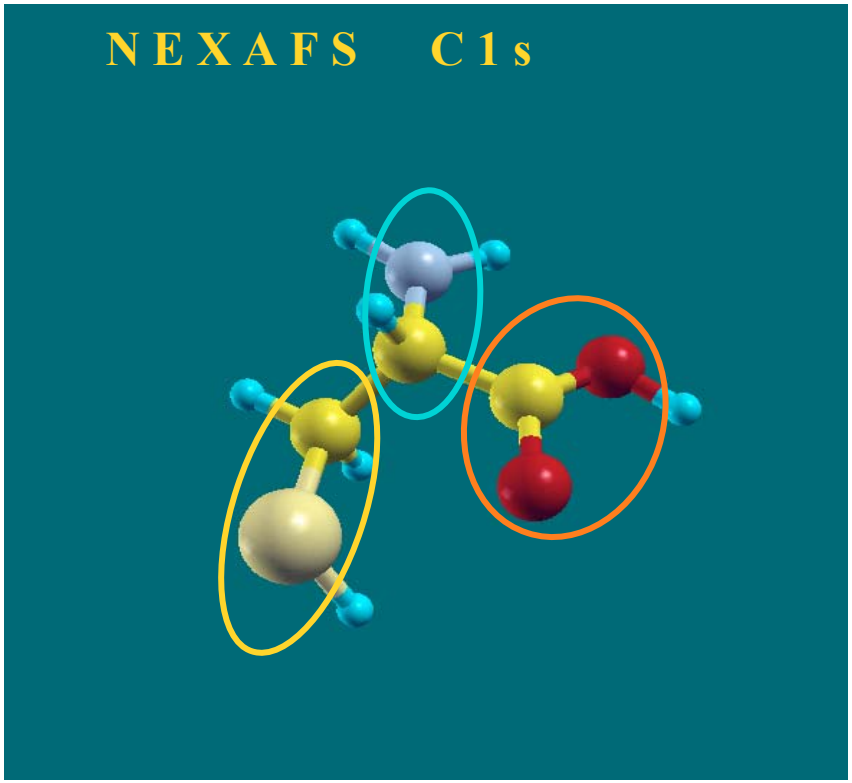


S-C peak evidence, S-C bond parallel to the surface

COO plane parallel to the surface

Other S-C and C-N related features

# The copper-phthalocyanine (CuPC) molecule

Electronic structure: delocalized π
Gap in the visible energy region

Conduction in molecular solid is anisotropic
Self-assembling

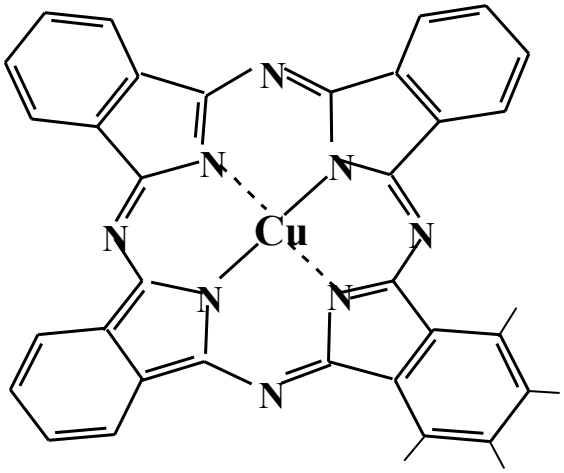


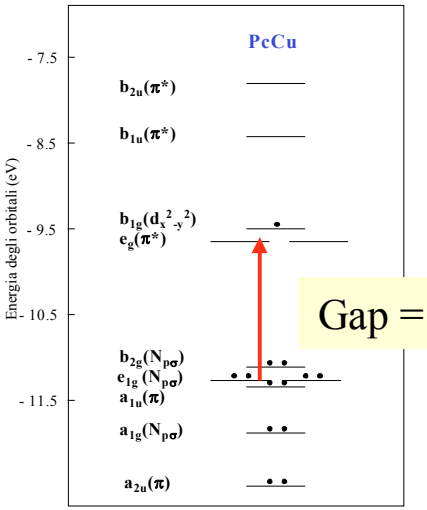


Gap = 1.9 eV

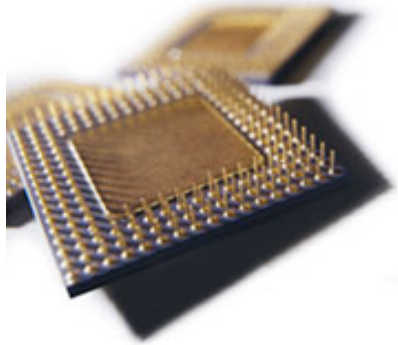

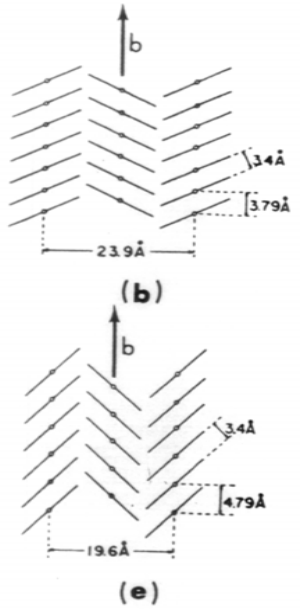

## The CuPc/Au(110) system

## Au(110) cell structure: out of plane X-ray diffraction

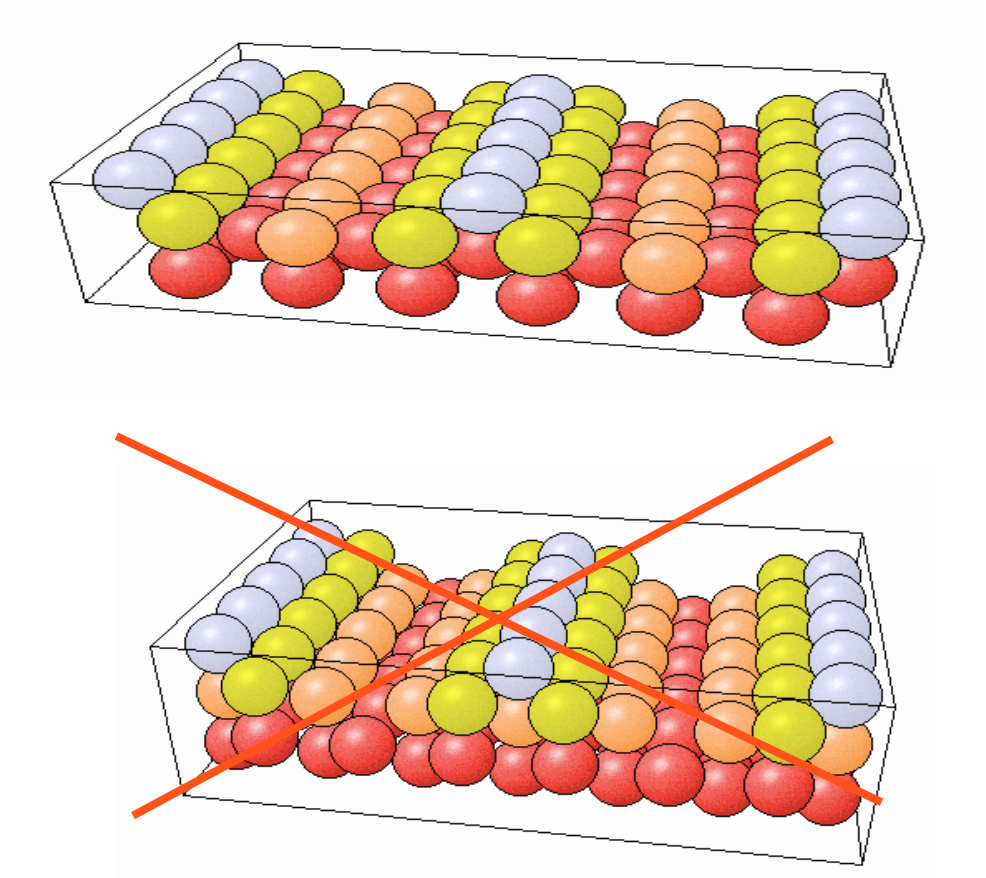

(0 , 3) rodscan

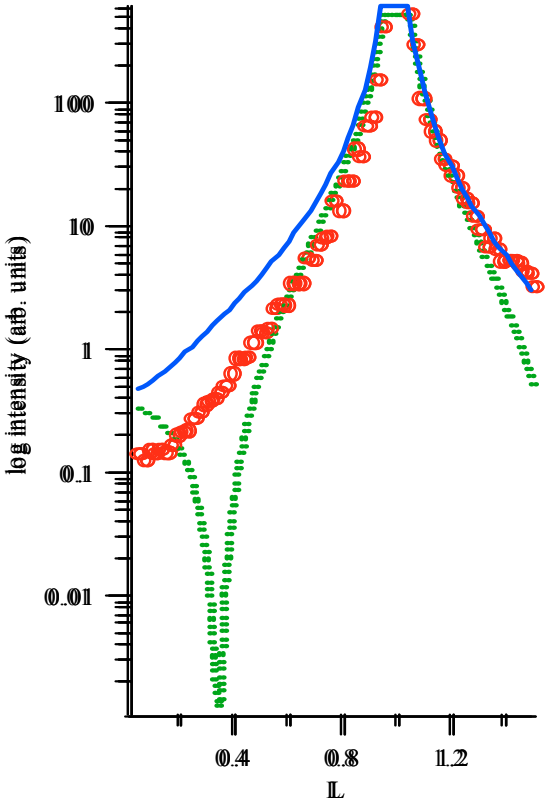


According to theory most energetically favourable 1x3 reconstruction deep MR

Deep 1x3 reconstruction proposed for perylene and T6 on Au(110)

The CuPc/Au(110) system

# X-ray diffraction: ×3 phase rodscans

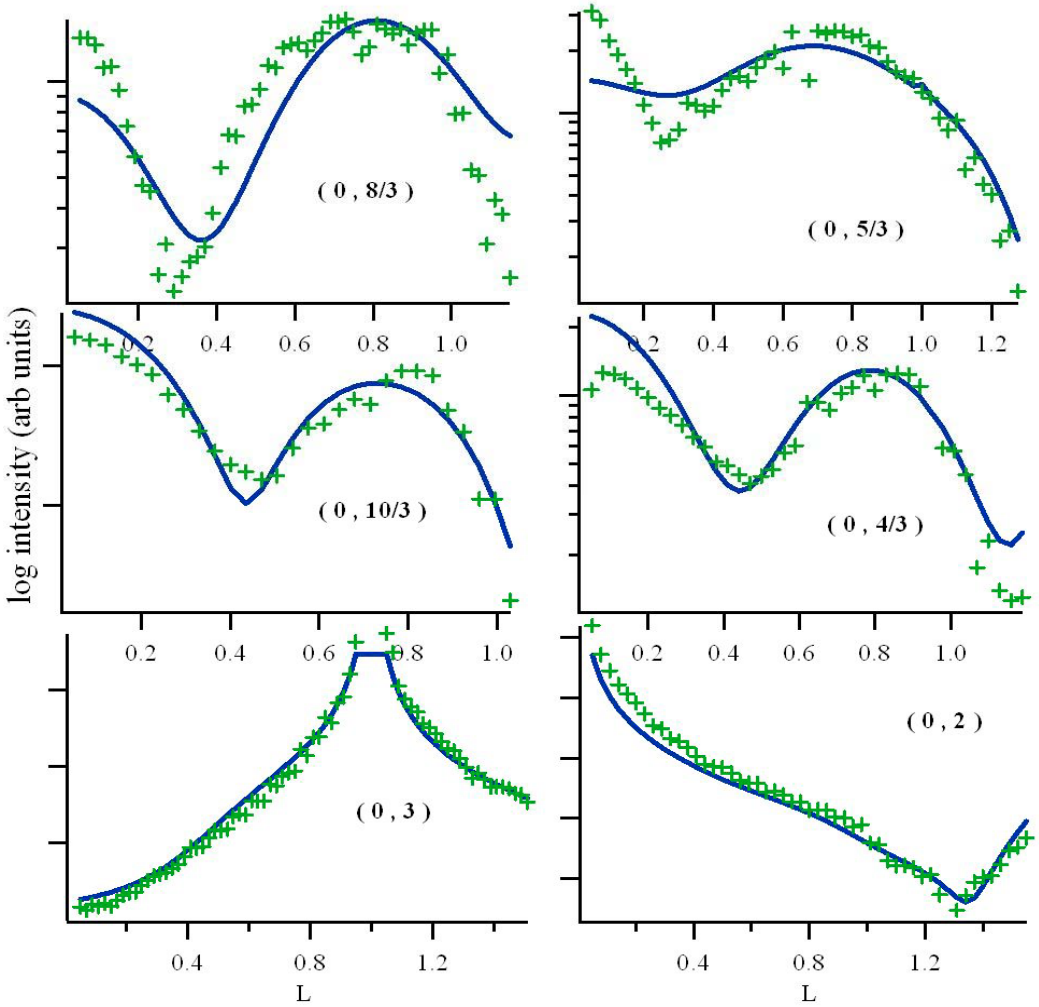


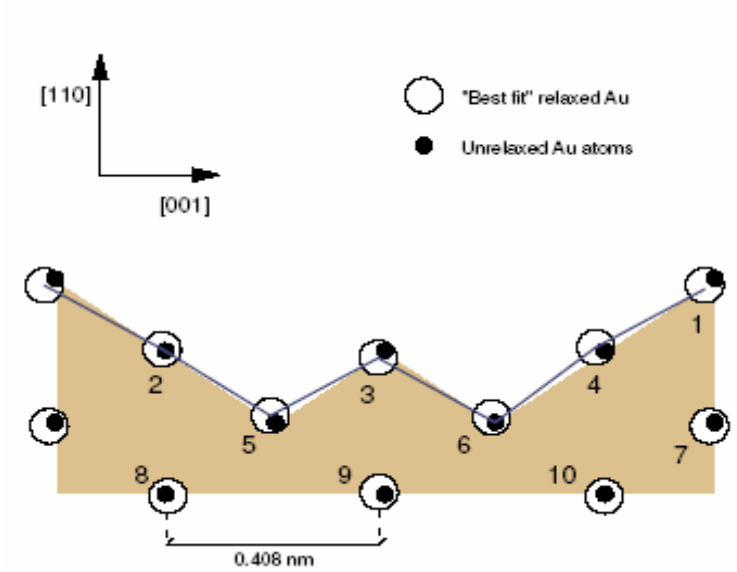


Shallow x3 reconstruction

The cell is asymmetric

Asymmetric molecule orientation

# Molecular orientation

The $2p \rightarrow 3d x^2\text{-}y^2$ transition is strongly polarized in the molecular plane.
The corresponding white lines exhibit a strong dichroism.

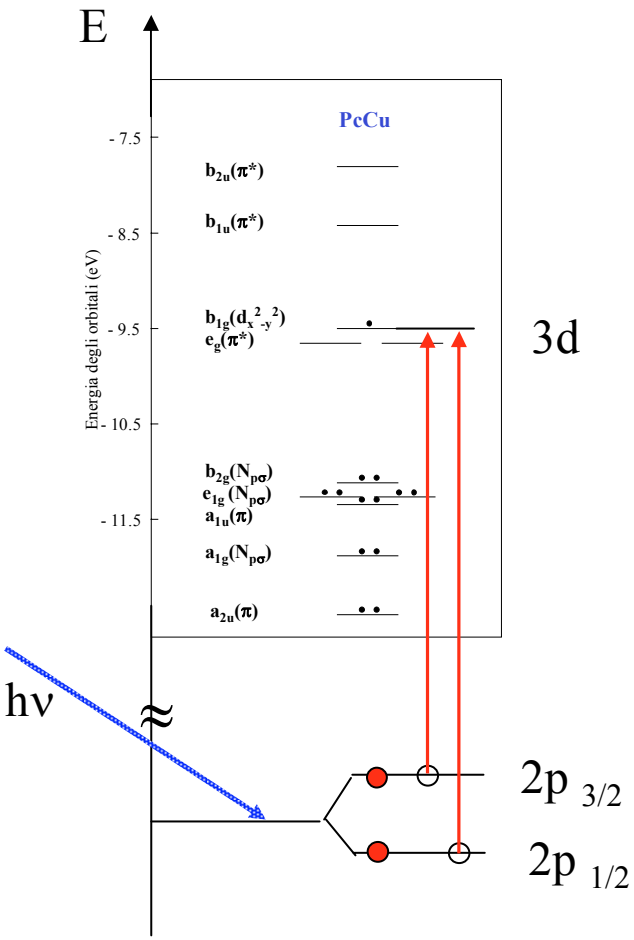


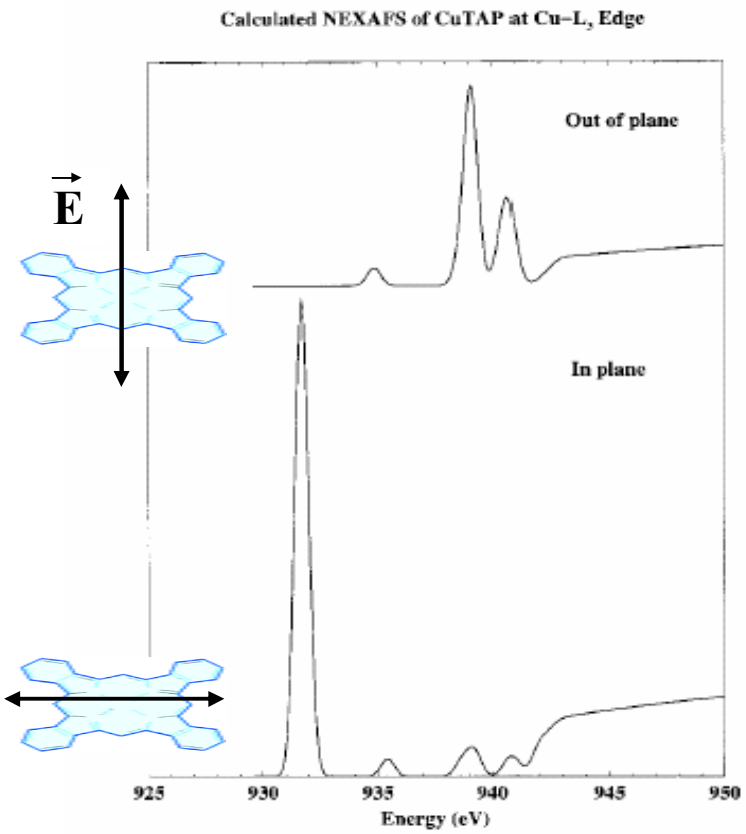


*Carniato et al.* PRB 63 85105

## The CuPc/Au(110) system

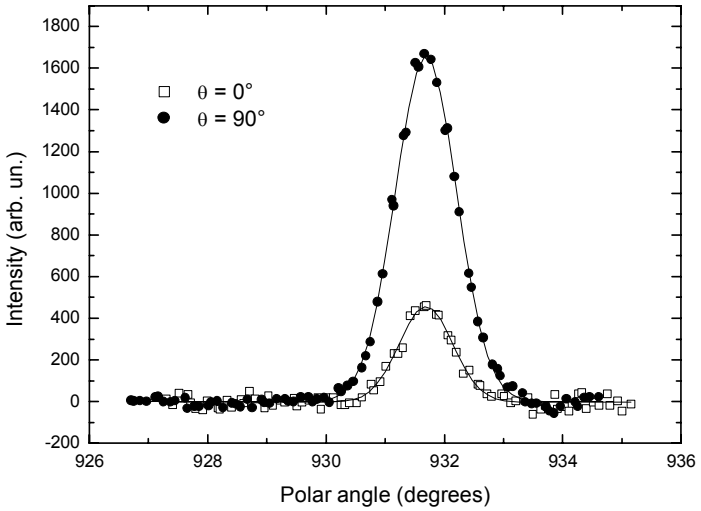


## Molecular orientation

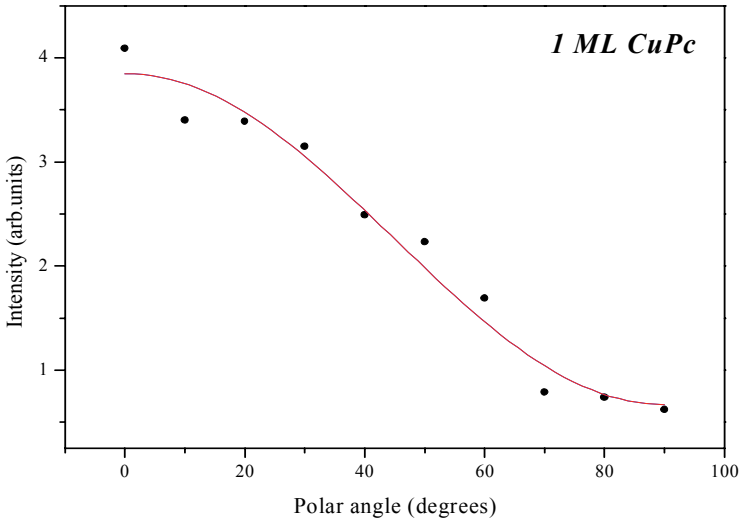


$I = S(1-|\sin\gamma \sin\alpha + \cos\gamma \sin\theta\cos\alpha|^2)$

$\alpha$=7° , incidence angle
$\theta$ polar angle
$\gamma$ molecules tilt angle

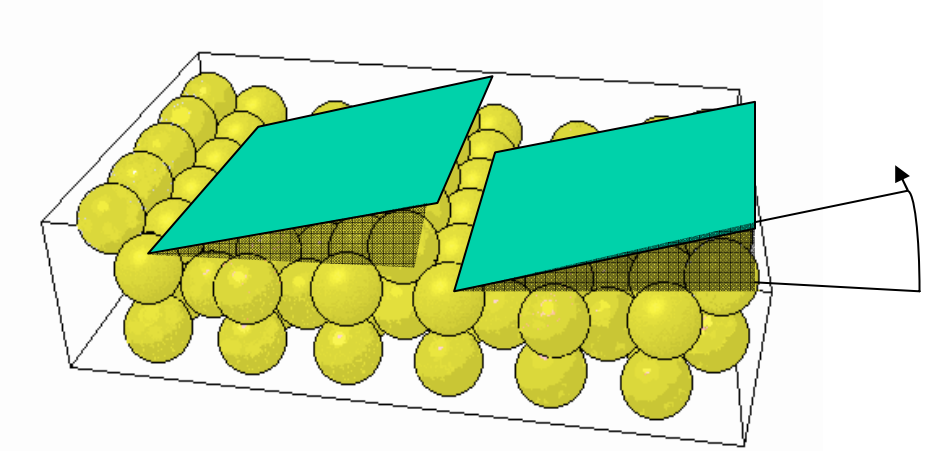

$\gamma$=32°

The molecule is 32 deg tilted with respect to the surface

## The CuPc/Au(110) system

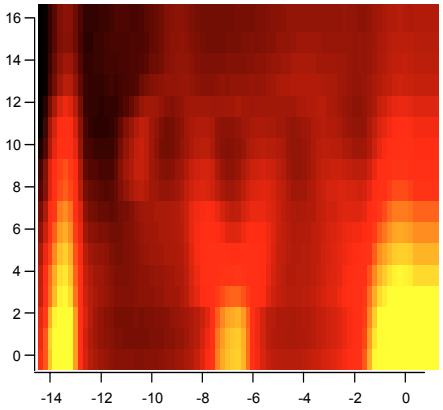


**× 3 phase**

× 5 phase

× 2 substrate phase

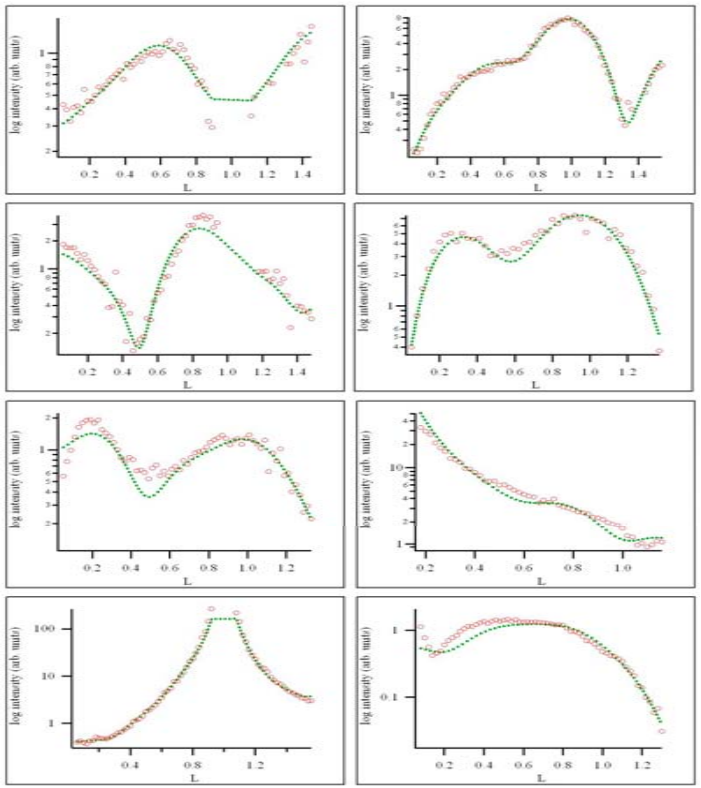

# The ×5 phase

- Shallow reconstructed ×5 cell
- Composed of ×3 and **×2 cells**
- Buckling of the third layer

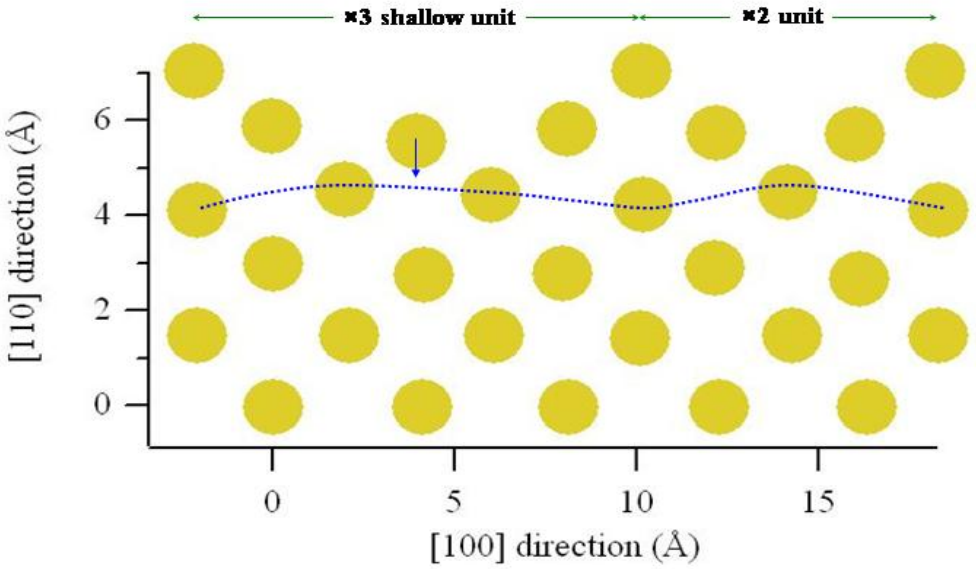

# Cu-phthalocyanine/Au(110)

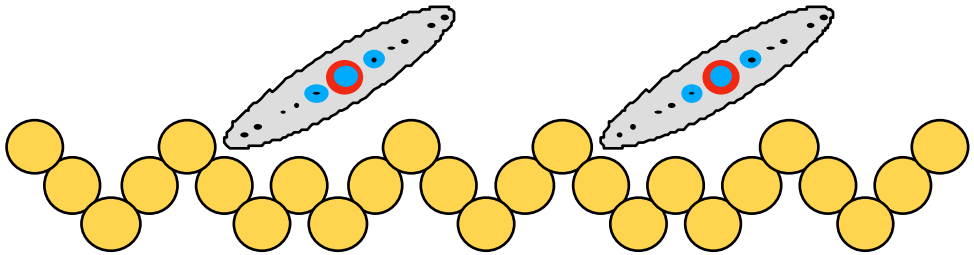

(5 x **5**)

3/5 ML

CHAIN-CHAIN REPULSION DRIVES Cu-Pc ARRAY PHASES

# Conclusions

Weaker interaction of CuPc on Au respect to Al substrate from spectroscopy (XPS, NEXAFS)

**but**

CuPc (1x2) MR reconstruction lifted; substrate reconstruct x5 and x3 (x5 composed of a x2 + x3 units)

x3 unit is a “shallow” MR reconstruction

x3 asymmetric cell (asymmetric atomic relaxations) from GIXD

Consistent with tilted geometry of the molecule from NEXAFS

CuPc molecules aligned along [1-10] direction long range order implies interaction between rows

At RT no long range order of the molecule for the x3 saturation phase observed from HAS.